

## Chapter 2

# The Cosmography

It is said that we live in the era of “precision cosmology”, and to some degree such a statement is correct. By the first years of the new millinium, the fundamental cosmological parameters had been constrained to precisions on the order of 10%. Though we will not discuss the deeper nature of each of the parameters, it is somewhat an embarrassing state of affairs that with great precision comes great ignorance. We know (or think we know) that the universe comprises 4% baryonic matter, 29% dark matter, 67% dark energy, is “flat” geometrically, and is presently expanding at the rate of  $70 \text{ km s}^{-1} \text{ Mpc}^{-1}$  with an acceleration rate of  $40 \text{ km s}^{-2} \text{ Mpc}^{-1}$ . However, we have no real understanding of the nature of dark matter, nor of dark energy, which is believed to be the source of the acceleration. That highlights the embarrassing fact that we only understand the fundamental nature of 4% of the constituents of the universe. This is the setting in which the study of quasar absorption lines operates.

One of the main consequences of having greater precision in the cosmological parameters is that various quasar absorption line researchers and research groups have begun to adopt a common set of values. This means that the computed distances, velocities, and projected separations of astronomical objects are now on a common metric. In the literature dating prior to the late 1990s, when precision was still only a distant hope, it was common that different researchers adopted their favored values, and these quantities ranged up to a factor of two in uncertainty. For example, Hubble’s constant was constrained to be in the range  $H_0 = 50\text{--}100 \text{ km s}^{-1} \text{ Mpc}^{-1}$ ; this important parameter of the current cosmological expansion rate appears to various powers in such quantities as cosmological distances, densities, transverse separations, velocity differences, and normalization constants in distribution functions. As, such, undesirable conversion between previous

works was (and still is) required.

In this chapter, we introduce the Robertson–Walker metric, which is the standard metric for measuring space and time intervals in the context of relativistic dynamics of an expanding spacetime geometry as described by Einstein’s General Relativity. Einstein’s field equations are presented and then rewritten in terms of the modern cosmological parameters. The present day values of these parameters are briefly discussed. The formalism of the dynamic spacetime geometry is then inserted into the Robertson–Walker metric, from which straight forward expressions for time and distance elements are derived. The goal is to introduce and clarify the origin of many expressions base upon the cosmological setting that are employed in the analysis of quasar absorption line studies. It is common that the absorbing gas is studied in relation to luminous objects, such as galaxies. Thus, we also discuss the relationship between luminosity and magnitude for emitting objects at cosmological distances. We include a brief discussion of photometric systems and present the so-called  $K$  correction.

Good resources for further details on the basic formalism of cosmological expansion are J. Peeble’s book, “Principles of Physical Cosmology” and the article “The Cosmological Constant” by Carrol, Press, & Turner (1992). An excellent distillation can be found in D. Hogg’s paper, “Distance Measures in Cosmology” (astro-ph/9905116). A more general, and easily accessible assessment of the currently adopted cosmology can be found in a series of five papers by M. Turner (Turner, 2001a,b, 2002a,b,c).

## 2.1 The Metric

The metric supplies the formalism for computing temporal and spatial coordinate positions and separations in a given generalized geometry, of which three-dimensional Euclidean geometry is a special case. Even if the geometry is not static, the metric can be applied with little generalization if the dynamics of the geometry are isotropic and homogenous. Consider a static geometric space with arbitrary curvature, where the radius of curvature is

$$R^2 = x^2 + y^2 + z^2 + w^2 = r^2 + w^2 \quad (2.1)$$

where  $r$  is the spatial distance and  $w$  represents the departure from Euclidean distances due to the curvature. The hyperspace can be mapped to

spherical coordinates with the observer at the origin, giving

$$\begin{aligned}
 x &= r \sin \theta \cos \phi \\
 y &= r \sin \theta \sin \phi \\
 z &= r \cos \theta \\
 w &= \sqrt{R^2 - r^2},
 \end{aligned} \tag{2.2}$$

where  $\theta$  and  $\phi$  are the polar and azimuthal angles in the spherical coordinate system, with  $0 \leq \theta \leq \pi$  and  $0 \leq \phi \leq 2\pi$ . The distance element is

$$dl^2 = dx^2 + dy^2 + dz^2 + dw^2. \tag{2.3}$$

In an isotropic and homogeneous dynamic spacetime geometry, the full metric, which is the “distance” element between events in spacetime, is written

$$ds^2 = c^2 dt^2 - a^2(t) dl^2, \tag{2.4}$$

where  $dt$  is the time element,  $c$  is the speed of light, giving the temporal element  $d\tau$  between events, and  $dl$  is the spatial distance element. The function of proportionality,  $a(t)$ , is the time dependent scale factor that accounts for isotropic and homogenous dynamics of the spatial element (i.e., expansion or contraction). The evolution of the scale factor is governed by the dynamics of the spacetime geometry, whereas the metric provides the means to compute the relative locations of and separations between spacetime events.

The Robertson–Walker metric has become the standard for describing the spacetime geometry of the expanding universe. Here, we outline its derivation. The spatial and curvature elements are written

$$\begin{aligned}
 dx &= dr \sin \theta \cos \phi + r(\cos \theta \cos \phi d\theta - \sin \theta \sin \phi d\phi) \\
 dy &= dr \sin \theta \sin \phi - r(\cos \theta \sin \phi d\theta + \sin \theta \cos \phi d\phi) \\
 dz &= dr \cos \theta - r \sin \theta d\theta \\
 dw &= \frac{r dr}{w}.
 \end{aligned} \tag{2.5}$$

After some manipulation, the generalized spatial distance element can be written

$$dl^2 = \frac{R^2 dr^2}{w} + r^2 d\psi^2 \tag{2.6}$$

where  $d\psi^2 = d\theta^2 + \sin^2 \theta d\phi$ . Of course, if the geometry is flat,  $w = dw = 0$  and the distance element is the Euclidian element,  $dl^2 = dr^2 + r^2 d\psi^2$ .

In the case of positive curvature, it is customary to further parameterize the radius of curvature by an “angle”  $\chi$  that represents a co-moving coordinate,

$$R^2 = r^2 + w^2 = R^2 \sin^2 \chi + R^2 \cos^2 \chi. \quad (2.7)$$

For negative curvature, we incorporate the fact that the radius of curvature is imaginary. In this case, the curvature is  $iR$ , which gives  $R^2 < 0$ , and the co-moving coordinate is  $i\chi$ . From this form of parameterization, we obtain  $r = iR \sin i\chi = iR \sinh \chi$ , and  $w = iR \cos i\chi = iR \cosh \chi$ . The generalized parameterization is summarized as follows:

$$r = \begin{cases} R \sin \chi & \text{positive} & k = +1 \\ R\chi & \text{flat} & k = 0 \\ R \sinh \chi & \text{negative} & k = -1, \end{cases} \quad (2.8)$$

and

$$w = \begin{cases} iR \cos \chi & \text{positive} & k = +1 \\ 0 & \text{flat} & k = 0 \\ iR \cosh \chi & \text{negative} & k = -1. \end{cases} \quad (2.9)$$

Though  $\chi$  is not a direct observable, it can be computed in terms of observables. The radius of curvature is commonly expressed

$$\kappa = \frac{1}{R^2}, \quad (2.10)$$

from which the unitless curvature constant,  $k$ , is defined:

$$k = \text{sign}(\kappa) = \begin{cases} +1 & (1/R)^2 > 0 & \text{positive} \\ 0 & (1/R)^2 = 0 & \text{flat} \\ -1 & (1/iR)^2 < 0 & \text{negative.} \end{cases} \quad (2.11)$$

Consider the positive curvature case; substituting Eqs. 2.8 and 2.9 for  $R$  in Eq. 2.6,

$$\begin{aligned} dl^2 &= R^2 \frac{dr^2}{w^2} + r^2 d\psi^2 \\ &= R^2 \frac{R^2 \cos^2 \chi d\chi^2}{R^2 \cos^2 \chi} + R^2 \sin^2 \chi d\psi^2 \\ &= R^2 (d\chi^2 + \sin^2 \chi d\psi^2), \end{aligned} \quad (2.12)$$

where the similar result, holds for the negative curvature case

$$\begin{aligned} dl^2 &= (iR)^2 \frac{(iR)^2 \cosh^2 \chi d\chi^2}{(iR)^2 \cosh^2 \chi} + (iR)^2 \sinh^2 \chi d\psi^2 \\ &= -R^2 (d\chi^2 + \sinh^2 \chi d\psi^2). \end{aligned} \quad (2.13)$$

Recall that  $R^2 < 0$ , so that  $dl > 0$  holds true. For the flat case, we have

$$dl^2 = R^2 (d\chi^2 + \chi^2 d\psi^2). \quad (2.14)$$

The full Robertson–Walker metric can then be written in the compact form for positive, flat, and negative curvature,

$$ds^2 = c^2 dt^2 - a^2(t) |R^2| \left[ d\chi^2 + f_k^2(\chi) d\psi^2 \right], \quad (2.15)$$

where the radius of curvature can be written as an absolute value to eliminate modifying the sign in front of the spatial element, and where

$$f_k(\chi) = \begin{cases} \sin \chi & \text{positive } k = +1 \\ \chi & \text{flat } k = 0 \\ \sinh \chi & \text{negative } k = -1. \end{cases} \quad (2.16)$$

Photons travel along so-called geodesics, defined by  $ds = 0$ . For radial (line of sight to the observer at the origin) distances  $d\psi = 0$ , so that the metric is greatly simplified to

$$cdt = a(t) |R| d\chi. \quad (2.17)$$

The proper distance is defined along the surface of constant time, i.e.,  $dt = 0$ . For radial distances  $d\psi = 0$ , so that the metric is greatly simplified to

$$dl = a(t) |R| d\chi. \quad (2.18)$$

Distances between events observed at different angles must include the non-zero term  $f_k(\chi) d\psi$ . The Robertson–Walker metric will be applied throughout this chapter to derive distances and velocities to objects carried by cosmological expansion. In order to do so, we need to know how to determine the time evolution of the scale factor,  $a(t)$ , parameterize the radius of curvature,  $R$ , and express the co-moving coordinate,  $\chi$ , in terms of observables.

## 2.2 Relativistic Dynamics

The dynamics of the scale factor is governed by Einstein's General Relativity field equations, in which the dynamics of spacetime are coupled to the energy density and pressure of the material universe. The temporal component of the spacetime dynamics is given by

$$3\frac{\dot{a}^2(t)}{a^2(t)} + 3\frac{\kappa c^2}{a^2(t)} - \Lambda c^2 = 8\pi G\rho(t), \quad (2.19)$$

and the spatial component is given by

$$-2\frac{\ddot{a}(t)}{a(t)} - \frac{\dot{a}^2(t)}{a^2(t)} - \frac{\kappa c^2}{a^2(t)} + \Lambda c^2 = 8\pi Gp(t), \quad (2.20)$$

where  $\ddot{a}(t)$  is the acceleration of the expansion at time  $t$ ,  $\dot{a}(t)$  is the expansion velocity,  $a(t)$  is the scale factor,  $\rho(t)$  is the energy–matter density,  $p(t)$  is the pressure, and  $\Lambda$ , known as the cosmological constant, is a negative density/pressure term (originally introduced to force a static solution!). A modern interpretation of  $\Lambda$  is that it is related to the energy of the vacuum (presently thought to be a non–evolving quantity). Note that the units of Eqs 2.19 and 2.20 are the inverse square of time ( $s^{-2}$ ).

Rearranging Eq. 2.19, and substituting Eq. 2.19 into Eq. 2.20, we have the familiar forms of the field equations,

$$\begin{aligned} \frac{\dot{a}^2(t)}{a^2(t)} &= \frac{8\pi G\rho(t)}{3} - \frac{\kappa c^2}{a^2(t)} + \frac{\Lambda}{3} \\ \frac{\ddot{a}(t)}{a(t)} &= -\frac{4\pi G}{3} \left[ \rho(t) + 3p(t) \right] + \frac{\Lambda}{3} \end{aligned} \quad (2.21)$$

A schematic of the field equations (Eq. 2.21) is presented in Fig. 2.1. At time  $t$ , a representative cube of space with scale  $a(t)$  is expanding at the rate  $\dot{a}(t)$ . The time domain is  $0 \leq t \leq t_0$ , where  $t_0$  is the present time (age) of the universe. Note that  $\dot{a}(t < t_0) > 0$ ;  $a(t)$  has been increasing with time and was always smaller at earlier times. The rate of change in  $\dot{a}(t)$  is  $\ddot{a}(t)$ , which can in principle be positive or negative (deceleration, as shown). It is the physical response of the energy density and pressure to an expanding geometry that will govern the specific time evolution of the scale factor.

The total energy density and pressure is the sum of various forms,

$$\rho(t) = \sum_i \rho_i(t) \quad p(t) = \sum_i p_i(t), \quad (2.22)$$

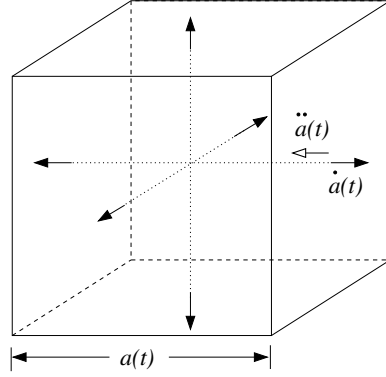


Figure 2.1: — A representation of the cosmological expansion. The scale factor,  $a(t)$ , parameterizes the evolving metric of space between two arbitrary points as a function time,  $t$ . The expansion is quantified by its rate,  $\dot{a}$  and by its acceleration,  $\ddot{a}$ .

where the indices denote

$$\begin{aligned} i = 1 & \quad \rho_m(t) & \text{matter} \\ i = 2 & \quad \rho_r(t) & \text{radiation} \\ i = 3 & \quad \rho_\Lambda(t) & \text{cosmological constant.} \end{aligned} \quad (2.23)$$

(Though the cosmological constant appears explicitly in the field equations, Eq. 2.21, we will see that it behaves as a negative energy density and pressure and can be formally treated in that fashion).

In order to complete the description of the relativistic dynamics, we must incorporate the continuity equation, which describes the conservation of matter–energy in a dynamic volume element, and the equation of state relating the density and pressure of the matter–energy “fluid”. The continuity equation can be derived via differentiation and manipulation of Eqs. 2.19 and 2.20,

$$\dot{\rho}_i(t) - 3 \frac{\dot{a}(t)}{a(t)} [\rho_i(t) + p_i(t)] = 0. \quad (2.24)$$

The equation of state for a relativistic fluid is

$$p_i(t) = \omega_i \rho_i(t), \quad (2.25)$$

where  $\omega_i = c_s = \sqrt{dp_i/d\rho_i}$  is the sound speed in the fluid. The values of  $\omega_i$  are

$$\omega_i = \begin{cases} 0 & \text{matter} \\ 1/3 & \text{radiation} \\ -1 & \text{cosmological constant.} \end{cases} \quad (2.26)$$

Substituting Eq. 2.25 into Eq. 2.24 gives

$$\dot{\rho}_i(t) = 3\rho_i(t) \frac{\dot{a}(t)}{a(t)} (1 + \omega_i). \quad (2.27)$$

for each component. Integrating gives

$$\rho_i(t) = \rho_{0,i} \left( \frac{a(t)}{a_0} \right)^{-3(1+\omega_i)}, \quad (2.28)$$

where  $\rho_{0,i}$  is the energy density of the  $i$ th form at the present time,  $t = t_0$ , and  $a_0$  is the scale factor at the present time. Eq. 2.28 describes the time evolution of the matter–energy density in a geometry undergoing isotropic, homogeneous contraction or expansion.

Writing out the field equations (Eq. 2.21) in terms of the sum of the matter–density components, gives

$$\frac{\ddot{a}(t)}{a(t)} = -\frac{4\pi G}{3} \sum_i (1 + 3\omega_i) \rho_i(t) \quad (2.29)$$

$$\frac{\dot{a}^2(t)}{a^2(t)} = \frac{8\pi G}{3} \sum_i \rho_i(t) - \frac{\kappa c^2}{a^2(t)} \quad (2.30)$$

Carrying out the summations and applying Eq. 2.26, we have

$$\frac{\ddot{a}(t)}{a(t)} = -\frac{8\pi G}{3} \left[ \frac{\rho_m}{2} \left( \frac{a(t)}{a_0} \right)^{-3} + \rho_r \left( \frac{a(t)}{a_0} \right)^{-4} - \rho_\Lambda \right], \quad (2.31)$$

$$\frac{\dot{a}^2(t)}{a^2(t)} = \frac{8\pi G}{3} \left[ \rho_m \left( \frac{a(t)}{a_0} \right)^{-3} + \rho_r \left( \frac{a(t)}{a_0} \right)^{-4} + \rho_\Lambda \right] - \frac{\kappa c^2}{a^2(t)} \quad (2.32)$$

where  $\rho_m = \rho_{0,m}$  is the matter density at the present time  $\rho_r = \rho_{0,r}$  is the radiation energy at the present time, and  $\rho_\Lambda = \rho_{0,\Lambda}$  is the energy density of the cosmological constant at the present time. From inspection of Eq. 2.21, we see that

$$\Lambda c^2 = 8\pi G \rho_\Lambda. \quad (2.33)$$

## 2.3 Parameterized Cosmology

Since  $a(t)$  appears in the Robertson–Walker metric, it is clear that the time evolution of distance intervals are linked to the field equations through the relativistic dynamics of the expansion of the universe. However, there are quantities appearing in the field equations whose values must be constrained by observations. These include  $\rho_m$ ,  $\rho_r$ ,  $\rho_\Lambda$ , and the radius of curvature  $\kappa = 1/R^2$ .



### 2.3.1 Parameterizing the Dynamics

Evaluation of Eq. 2.32 at the current epoch, i.e.,  $t = t_0$ , provides convenient parameterization of the present day energy densities and has the added benefit of yielding an expression for the radius of the present day curvature in terms of the present day observable quantities. We have,

$$H_0^2 \equiv \frac{\dot{a}_0^2}{a_0^2} = \frac{8\pi G}{3} [\rho_m + \rho_r + \rho_\Lambda] - \frac{\kappa c^2}{a_0^2}, \quad (2.34)$$

where the present day velocity of expansion per scale length is defined as the Hubble constant,  $H_0 = \dot{a}_0/a_0$ . Dividing Eq. 2.34 by  $H_0^2$  gives

$$1 = \frac{8\pi G}{3H_0^2} [\rho_m + \rho_r + \rho_\Lambda] - \frac{\kappa c^2}{a_0^2 H_0^2}. \quad (2.35)$$

The form of Eq. 2.35 is the origin of the well-known present day dimensionless cosmological density parameters

$$\begin{aligned} \Omega_m &= \frac{8\pi G \rho_m}{3H_0^2} \\ \Omega_r &= \frac{8\pi G \rho_r}{3H_0^2} \\ \Omega_\Lambda &= \frac{\Lambda c^2}{3H_0^2} \\ \Omega_k &= \frac{-\kappa c^2}{a_0^2 H_0^2}. \end{aligned} \quad (2.36)$$

Employing this notation, Eq. 2.35 is rewritten

$$\Omega_m + \Omega_r + \Omega_\Lambda + \Omega_k = 1. \quad (2.37)$$

Given that  $\Omega_k$  depends upon the radius of curvature, we can rearrange Eq. 2.37 to obtain  $R$  in terms of  $\Omega_m$ ,  $\Omega_r$ , and  $\Omega_\Lambda$ ,

$$\Omega_k = \frac{-\kappa c^2}{a_0^2 H_0^2} = 1 - (\Omega_m + \Omega_r + \Omega_\Lambda). \quad (2.38)$$

$$\begin{aligned} \Omega_k < 0 & \quad (k = +1, \text{ positive, closed}) \\ \Omega_k = 0 & \quad (k = 0, \text{ flat}) \\ \Omega_k > 0 & \quad (k = -1, \text{ negative, open}), \end{aligned} \quad (2.39)$$

where  $k = \text{sign}(\kappa) = \text{sign}(1/R^2)$ . We have

$$R^2 = \left( \frac{c}{a_0 H_0} \right)^2 \frac{1}{\Omega_k} = \left( \frac{c}{a_0 H_0} \right)^2 \left[ (1 - \Omega_m - \Omega_r - \Omega_\Lambda) \right]^{-1} \quad (2.40)$$

The cosmological density parameters given in Eq. 2.36 apply to the present epoch. From the integrated continuity equation (Eq. 2.28), we recall that the cosmic density of matter has steadily decreased as the universe expands, such that  $\rho_m(t) = \rho_m(a_0/a(t))^3$  whereas radiation energy density evolves as  $\rho_r(t) = \rho_r(a_0/a(t))^4$ . The cosmological constant has no dependence on the evolution of the scale factor (at least that is the current expectation). On the other hand, the curvature is in proportion to  $a^2(t)$ , and decreases with time according to

$$-\frac{\kappa c^2}{a_0^2} \left( \frac{a_0}{a(t)} \right)^2. \quad (2.41)$$

In terms of the dimensionless density parameters, the time evolution is summarized to be

$$\begin{aligned} \Omega_m(t) &= \left( \frac{a_0}{a(t)} \right)^3 \Omega_m(t_0) \\ \Omega_r(t) &= \left( \frac{a_0}{a(t)} \right)^4 \Omega_r(t_0) \\ \Omega_\Lambda(t) &= \Omega_\Lambda(t_0) \\ \Omega_k(t) &= \left( \frac{a_0}{a(t)} \right)^2 \Omega_k(t_0), \end{aligned} \quad (2.42)$$

where  $t_0$  is the present time (age) of the universe and has been explicitly written in Eq. 2.42 for clarification.

Though the ratio of radiation energy density to matter energy density,  $\rho_r(t)/\rho_m(t)$  was unity when  $a_0/a(t) = 1000$  (an epoch called recombination), the present day value is roughly  $\rho_r/\rho_m \simeq 10^{-3}$  and it is decreasing. Since  $\Omega_r$  equals only 0.1% of  $\Omega_m$ , it is common practice to drop  $\Omega_r$  from the field equations. Recall that the ratio scales as  $\rho_r/\rho_m \propto a_0/a(t)$ , which can be used to estimate the scale factor at which radiation energy density begins to make at a given percent contribution. Quasar spectroscopy is firmly planted in the domain  $a_0/a(t) < 10$  (actually more like  $a_0/a(t) \leq 7$ ). Thus, the radiation energy density can be neglected for such work.

The full expression of the field equations, Eqs. 2.31 and 2.32 can now be highly simplified into a compact form. The expansion velocity per unit scale length is written

$$H(t) = \frac{\dot{a}(t)}{a(t)} = H_0 E(t), \quad (2.43)$$

and the acceleration per unit scale length is written

$$\dot{H}(t) = \frac{\ddot{a}(t)}{a(t)} = H_0 E'(t). \quad (2.44)$$

In terms of the dimensionless cosmological parameters, the expression for  $E(t)$  is

$$E(t) = \left[ \Omega_m(t) + \Omega_k(t) + \Omega_\Lambda \right]^{1/2}, \quad (2.45)$$

which is explicitly written

$$E(t) = \left[ \Omega_m \left( \frac{a_0}{a(t)} \right)^3 + \Omega_k \left( \frac{a_0}{a(t)} \right)^2 + \Omega_\Lambda \right]^{1/2}, \quad (2.46)$$

where  $\Omega_r$  is neglected, and where  $E(t_0) = 1$ , giving the current day relationship

$$\Omega_m + \Omega_k + \Omega_\Lambda = 1. \quad (2.47)$$

The expression for  $E'(t)$  is

$$E'(t) = \Omega_\Lambda - \frac{1}{2}\Omega_m(t) = \Omega_\Lambda - \frac{1}{2}\Omega_m \left( \frac{a_0}{a(t)} \right)^3 \quad (2.48)$$

where  $\Omega_r$  is neglected. The range of  $E(t)$  is  $E(t_0) = 1$  and  $E(t < t_0) > 1$ . The allowed range of  $E'(t)$  is, in principle,  $-\infty \leq E'(t) \leq \infty$ .

Eq. 2.46 is substituted into Eq. 2.43 to obtain the time evolution of the expansion velocity per unit scale length,

$$\frac{\dot{a}(t)}{a(t)} = H_0 \left[ \Omega_m \left( \frac{a_0}{a(t)} \right)^3 + \Omega_k \left( \frac{a_0}{a(t)} \right)^2 + \Omega_\Lambda \right]^{1/2}, \quad (2.49)$$

and Eq. 2.48 is substituted into Eq. 2.44 to obtain the time evolution of the expansion acceleration per unit scale length,

$$\frac{\ddot{a}(t)}{a(t)} = H_0 \left[ \Omega_\Lambda - \frac{1}{2}\Omega_m \left( \frac{a_0}{a(t)} \right)^3 \right]. \quad (2.50)$$

### 2.3.2 Friedmann Cosmology, $\Lambda = 0$

On account that the Friedmann Cosmology has been applied often in the scientific literature prior to the year 2000, it is useful to review the expansion evolution and commonly used cosmological parameters for this model. By definition,  $\Lambda = 0$ . Thus, Eq 2.45 reduces to

$$E(t) = \left[ \Omega_m \left( \frac{a_0}{a(t)} \right)^3 + \Omega_k \left( \frac{a_0}{a(t)} \right)^2 \right]^{1/2}, \quad (2.51)$$

and Eq 2.48 reduces to

$$E'(t) = -\frac{1}{2} \Omega_m \left( \frac{a_0}{a(t)} \right)^3, \quad (2.52)$$

Applying the historical use of  $\Omega_0 = 1 - \Omega_k$  and the relation  $\Omega_m + \Omega_k = 1$ , yields

$$\Omega_0 = \Omega_m. \quad (2.53)$$

That is, in a Friedmann Cosmology, the curvature of the universe was dependent strictly upon the matter density parameter. It has been a long time convention to write  $\Omega_0 = \rho_m / \rho_c$ , where

$$\rho_c = \frac{3H_0^2}{8\pi G} = 1.88h^2 \times 10^{-29} \text{ g cm}^{-3}, \quad (2.54)$$

defines the critical matter density for which  $\Omega_0 = 1$  (zero curvature universe).

In this special case, the terms  $E(t)$  and  $E'(t)$  that describe the expansion velocity (Eq. 2.49) and acceleration (Eq. 2.50) depend only upon  $\Omega_0$ , which is often expressed as the deceleration parameter

$$q_0 \equiv -\frac{\ddot{a}_0 a_0}{\dot{a}_0^2} = \frac{1}{2} \Omega_0, \quad (2.55)$$

where  $\ddot{a}_0$ ,  $\dot{a}_0$ , and  $a_0$  are the acceleration, velocity, and scale factor of cosmological expansion at the present time.

Substituting Eqs. 2.53 and 2.55 into Eqs. 2.51 and 2.52, yields

$$E(t) = \frac{a_0}{a(t)} \left[ 1 + 2q_0 \left( \frac{a_0}{a(t)} - 1 \right) \right]^{1/2}, \quad (2.56)$$

where  $E(t_0) = 1$ , and

$$E'(t) = -q_0 \left( \frac{a_0}{a(t)} \right)^3, \quad (2.57)$$

which are substituted into Eq. 2.43 to obtain the time evolution of the expansion velocity per unit scale length and Eq. 2.44 to obtain the time evolution of the expansion acceleration per unit scale length.

### 2.3.3 Parameterizing the Metric

The compact form of the Robertson–Walker metric (Eq. 2.15) is

$$ds^2 = c^2 dt^2 - a^2(t) |R^2| \left[ d\chi^2 + f_k^2(\chi) d\psi^2 \right], \quad (2.58)$$

where  $f_k^2(\chi)$  is given by Eq. 2.16. Substituting Eq. 2.40 for  $R$ , we have

$$ds^2 = c^2 dt^2 - \frac{a^2(t)}{a_0^2} \frac{D_{\text{H}}^2}{\Omega_k} \left[ d\chi^2 + f_k^2(\chi) d\psi^2 \right], \quad (2.59)$$

where

$$D_{\text{H}} = \frac{c}{H_0}. \quad (2.60)$$

Rewriting the metric as

$$ds^2 = d\tau^2 - dl_r^2 - l_{\text{T}}^2 d\psi^2, \quad (2.61)$$

we can defined three main components,

$$\begin{aligned} d\tau &= c dt \\ dl_r &= \frac{a(t)}{a_0} \frac{D_{\text{H}}}{\sqrt{\Omega_k}} d\chi \\ l_{\text{T}} d\psi &= \frac{a(t)}{a_0} \frac{D_{\text{H}}}{\sqrt{\Omega_k}} f_k(\chi) d\psi \end{aligned} \quad (2.62)$$

where  $d\tau$  is the temporal element,  $dl_r$  is the radial proper distance element, and  $l_{\text{T}} d\psi$  is the transverse proper distance element. The radial proper distance elements is proportional to the co-moving coordinate element,  $d\chi$ , and the transverse proper distance element is proportional to the co-moving function  $f_k(\chi)$ , where the proportionality is given by the scale factor,  $a(t)/a_0$ . Recall that the time evolution of the scale factor is governed by the relativistic dynamics of spacetime [ $\dot{a}(t)/a(t) = H_0 E(t)$ , Eq. 2.43, and  $\ddot{a}(t)/a(t) = H_0 E'(t)$ , Eq. 2.44]. We can refine the distinction between proper and co-moving elements by writing

$$\begin{aligned} dl_r &= \frac{a(t)}{a_0} dD_c \\ l_{\text{T}} d\psi &= \frac{a(t)}{a_0} D_{\text{T}} d\psi \end{aligned} \quad (2.63)$$

which defines the co-moving distance element,  $dD_c$ , and the transverse co-moving distance  $D_T$ ,

$$\begin{aligned} dD_c &= \frac{D_H}{\sqrt{\Omega_k}} d\chi \\ D_T &= \frac{D_H}{\sqrt{\Omega_k}} f_k(\chi). \end{aligned} \quad (2.64)$$

Simple integration yields the radial co-moving distance  $D_c = (D_H/\sqrt{\Omega_k})\chi$ . The definitions of a transverse proper and co-moving distances are introduced for the description of non-radial intervals,  $ds$ , for which  $d\psi \neq 0$ ; they are applied to describe transverse separations of objects separated by an angle  $\theta = \int d\psi$  as observed from the origin.

The time element,  $dt$ , and scale factor element,  $da$ , are connected by the time derivative of the scale factor  $da/dt = \dot{a}(t)$ . We have

$$d\tau = cdt = c \frac{da}{\dot{a}(t)} = c \frac{a(t)}{\dot{a}(t)} \frac{da}{a(t)} = \frac{c}{H(t)} \frac{da}{a(t)} = D_H \frac{da}{a(t)E(t)}. \quad (2.65)$$

To obtain the proper distance element, we need to express the co-moving coordinate element,  $d\chi$ , in terms of the relativistic dynamics. Consider the metric for a photon traveling on a radial trajectory ( $d\psi = 0$ ) to the observer. Photons travel on geodesics, defined by  $ds = 0$ , which yields

$$d\tau = dl_r = \frac{a(t)}{a_0} \frac{D_H}{\sqrt{\Omega_k}} d\chi, \quad (2.66)$$

which, after substituting Eq. 2.65 for  $d\tau$ , gives

$$d\chi = a_0 \sqrt{\Omega_k} \frac{da}{a^2(t)E(t)}. \quad (2.67)$$

Integrating gives the co-moving coordinate

$$\chi = a_0 \sqrt{\Omega_k} \int_{a_0}^{a(t_e)} \frac{da}{a^2(t)E(t)}, \quad (2.68)$$

where  $t_e$  is the time at which the photon was emitted (or absorbed). Substituting Eqs. 2.67 and 2.68 into Eq. 2.64, yields the co-moving distances

$$\begin{aligned} D_c &= a_0 D_H \int_{a_0}^{a(t_e)} \frac{da}{a^2(t)E(t)} \\ D_T &= \frac{D_H}{\sqrt{\Omega_k}} f_k \left( \sqrt{\Omega_k} \frac{D_c}{D_H} \right). \end{aligned} \quad (2.69)$$

The above formalism has introduced the concepts of proper and co-moving distances. The interpretation for these will be discussed in § 2.8. As we have shown, the Robertson–Walker metric, and therefore time and distance intervals, can be written explicitly in terms of the cosmological parameters once the formalism of the field equations is substituted for the time evolution of  $a(t)$ . Armed with accurate values of  $H_0$ ,  $\Omega_m$ ,  $\Omega_k$ , and  $\Omega_\Lambda$  [all appearing in the product  $H_0 E(t)$ ], the computation of time and distance (and velocity) requires integration of a well behaved function. As presented above, the metric is written as a function of time, which means that it is still not expressed in terms of a direct observable, which is redshift. Thus, it will be important to recouch all time and distances as a function of redshift. This will be undertaken in the following sections.

## 2.4 $H_0$ and the Three $\Omega$ 's

Of the cosmological parameters appearing in the field equations, it is the *present day* expansion velocity per unit scale length, parameterized by the Hubble constant,  $H_0$  (units are  $\text{s}^{-1}$ ), which reigns supreme. The Hubble constant,  $H_0$ , is a factor of inverse square proportionality for each of the density parameters (Eq. 2.36), and is thus a very critical number. It is customary to parameterize the Hubble constant by the dimensionless parameter,  $h = H_0/100$ , where  $H_0$  is expressed in units  $\text{km s}^{-1} \text{Mpc}^{-1}$ .

From Eq. 2.42, recall that the three density parameters, matter energy density,  $\Omega_m$ , “dark energy” density,  $\Omega_\Lambda$ , and curvature density,  $\Omega_k$ , each have their own response to the expansion of space, which in turn responds back. It is required that we amend the matter energy density term. Observational constraints on baryonic matter and evidence for dark matter suggests that the total matter density is the sum of baryonic and non-baryonic (dark) components,

$$\Omega_m = \Omega_b + \Omega_{dm}. \quad (2.70)$$

Altogether, it has been the combined constraints from Big Bang Nucleosynthesis (BBN), measurements of the matter distribution of galaxies, and observations of the angular distributions of variations (anisotropy) in the cosmic background radiation (CMB), that have provided the coveted precision in the cosmological parameters. The measurement of deuterium abundances in quasar spectra has been applied to constrain the baryonic matter density in the context of the standard BBN model (e.g., Burles, Nollet, & Turner, 2001). The measured distribution of galaxies on large scales and in clusters from the Sloan Digital Sky Survey (Dodelson et al., 2002), the Canadian Network for Observational Cosmology (Carlberg et al., 1997),

and the 2-degree Field Galaxy Redshift Survey (Percival et al., 2002) have been applied to constrain the relative baryonic and dark matter distributions. CMB anisotropies, from experiments such as the *Cosmic Background Imager* (Sievers et al., 2003) the *Wilkinson Microwave Anisotropy Probe* (*WMAP*, Spergel et al., 2003), the two *Boomerang* flights (Netterfield et al., 2002), the *Degree Angular Scale Interferometer* (Halverson et al., 2002), and *MAXIMA* (Hanany et al., 2000), have been key to ushering in the age of precision cosmology by measuring most all cosmological parameters with great sensitivity.

However, often there are correlated dependencies, especially with the Hubble constant. BBN is sensitive to the baryon density,  $\Omega_b h^2$ , via the cosmic deuterium abundance. Both the baryon density,  $\Omega_b h$ , and the baryon to total matter ratio,  $\Omega_b/\Omega_m$ , can be measured in large volume galaxy surveys from the inhomogeneity of baryons, which trace the power spectrum of density fluctuations. The anisotropy of the CMB has separate dependencies upon  $\Omega_b h^2$  and  $\Omega_m h^2$ .

Evidence for a non-zero cosmological constant,  $\Lambda$ , began to emerge in the late 1990s. Measurements of supernovae magnitudes at cosmological distances did not match the expectations for  $\Lambda = 0$  (e.g., Perlmutter et al., 1999; Schmidt et al., 1998). The non-zero  $\Lambda$ , as it appears in Einstein's equation of General Relativity, acts as an acceleration term that counters gravitation deceleration; in its more recent epochs, the universe is accelerating its expansion. The energy density of the cosmological constant has been dubbed the "dark energy". As the supernova results began to be accepted, the reigning cosmological model to the twentieth century, known as the Friedmann Cosmology, i.e.,  $\Lambda = 0$ , was replaced with the so-called "New Cosmology", which we will refer to as  $\Lambda$  Cosmology.

From the above experiments, the maximum likelihood values for the "big four" cosmological parameters are (Turner, 2002d),

$$\begin{aligned}\Omega_m &= 0.33 \pm 0.04 && \text{total matter} \\ \Omega_k &= 0.03 \pm 0.03 && \text{curvature} \\ \Omega_\Lambda &= 0.67 \pm 0.06 && \text{dark energy} \\ h &= 0.70 \pm 0.03 && \text{Hubble constant}\end{aligned}\tag{2.71}$$

where the Hubble constant is the best value from the *WMAP* experiments, and where the dark energy is inferred from the supernova data and is obtained from Eq. 2.45, and where  $\Omega_m$  is broken into

$$\begin{aligned}\Omega_b &= 0.04 \pm 0.01 && \text{baryonic matter} \\ \Omega_{dm} &= 0.29 \pm 0.04 && \text{dark matter.}\end{aligned}\tag{2.72}$$



### 2.4.1 What was the Value of $q_0$ ?

Prior to the more precise measurements of the cosmological parameters, the value of  $\Omega_0$  was not well constrained. Observations at that time indicated that the matter density was closer to zero than to unity. Thus, many researchers favored a low-density or open Friedmann Cosmology, described by the two parameters

$$\begin{aligned}\Omega_0 &= 0.1 & \text{Low Density (open)} \\ q_0 &= 0.05,\end{aligned}\tag{2.73}$$

for which  $\Omega_k = 1 - \Omega_0 = 0.9$ . On the other hand, inflationary theory mandated  $\Omega_0 = 1$ , and many researchers favored the so called Einstein-de Sitter Cosmology, which is a zero curvature, matter dominated Friedmann Cosmology defined by

$$\begin{aligned}\Omega_0 &= 1.0 & \text{Einstein-de Sitter (flat)} \\ q_0 &= 0.5.\end{aligned}\tag{2.74}$$

This broad range of adopted cosmologies was further exasperated by poor constraints on the Hubble constant, which ranged between  $h = 0.5$ – $1.0$ ; this resulted in various research groups adopting different cosmologies when reporting their results and discussing the implications of their findings. For historical reasons, there were two camps with regard to the accepted value of  $h$ , the  $h \simeq 0.5$  camp and the  $h \simeq 1.0$  camp. Commonly, but not exclusively, those who applied the low-density Friedmann Cosmology, adopted  $h \simeq 0.5$ , where as those who applied the Einstein-de Sitter Cosmology adopted  $h = 1$ . This alone was a less than satisfying state of affairs. However, with the adoption of  $\Lambda$  Cosmology, there is now the added burden of translating quantities from the various Friedmann Cosmologies. The upside of course, is that most of the results presented in the literature since the year 2000 have adopted  $\Lambda$  Cosmology with the narrow range of Cosmological parameters.

## 2.5 Scale Factor and Redshift

The quantity called redshift is tied to the observable fractional “Doppler shift” of an object due to its being carried along the cosmological expansion. The redshift,  $z$ , measured in spectra is computed from

$$\frac{\lambda_o}{\lambda_e} = 1 + z,\tag{2.75}$$

where  $\lambda_o$  is the observed wavelength, and  $\lambda_e$  is the emitted rest-frame wavelength.

In fact, this redshift is not a Doppler shift at all— it is a recessional velocity redshift induced by the cosmological expansion of space. As a photon propagates over a very long period of cosmic time, the expansion of space also expands the photon wavelength (a sort of stretching of the light; photon wavelengths are proper distance intervals). This provides the physically correct interpretation of the redshift of distant objects.

Consider a photon of wavelength  $\lambda_e$  that was emitted at the time  $t_e$  when the scale factor of the universe was  $a(t_e)$ . As time passes,  $a(t)$  increases according to the behavior of Eq. 2.43 and 2.44 until the present epoch, at which time the scale factor is  $a_0$ . The photon wavelength will have been expanded such that  $\lambda_o/\lambda_e = a_0/a(t_e)$ . Substituting for  $\lambda_o/\lambda_e$  in Eq. 2.75, we see that the cosmological redshift is simply the ratio of the present day scale factor to the scale factor at the time the photon was emitted (or absorbed),

$$\frac{a_0}{a(t)} = 1 + z. \quad (2.76)$$

where the subscript denoting emission has been omitted. The redshift element is related to the scale factor element by

$$dz = \frac{a_0}{a^2(t)} da = (1 + z) \frac{da}{a(t)}. \quad (2.77)$$

Because of this relation between  $z$  and the direct observable quantity,  $\lambda_o/\lambda_e$ , redshift is a most convenient parameter for describing cosmological relationships. However, the factor  $1 + z$  should always be viewed as the ratio  $a_0/a(t)$ , and be thought of as the factor by which the universe has expanded since the photon was emitted (or absorbed) at the source. The redshift element,  $dz$ , should be viewed as the product of this ratio and the scale factor element normalized by the scale factor at the time of emission (or absorption).

As written above, Eq. 2.76 is the relationship between redshift and the scale factor at the current epoch. However, there are applications requiring knowledge of the redshift of an object at  $z_2$  as observed from another object at  $z_1$ , where  $z_2 > z_1$ . Denoting  $a_1 = a(t_1)$  and  $a_2 = a(t_2)$ , this is simply the ratio

$$\frac{(a_0/a_2)}{(a_0/a_1)} = \frac{1 + z_2}{1 + z_1} = \frac{a_1}{a_2} = 1 + z_{12}. \quad (2.78)$$

## 2.6 Dynamics and Redshift

Since the scale factor and observed redshift are interchangeable parameters, the equations describing cosmological expansion as a function of time (Eqs. 2.49 and 2.50) are conveniently expressed in terms of redshift. This provides the formalism for computing cosmological quantities in terms of a directly observable quantity. Substituting  $1 + z = a_0/a(t)$ , we can express the velocity per unit scale length as

$$\frac{\dot{a}(t)}{a(t)} = H(z) = H_0 E(z), \quad (2.79)$$

where

$$E(z) = \left[ \Omega_m (1+z)^3 + \Omega_k (1+z)^2 + \Omega_\Lambda \right]^{1/2}. \quad (2.80)$$

Eq. 2.79 defines the Hubble constant,  $H(z) = H_0 E(z)$ , as measured by a hypothetical observer at redshift  $z$ . Following the same substitution, the acceleration per unit scale length is expressed

$$\frac{\ddot{a}(t)}{a(t)} = \dot{H}(z) = H_0 E'(z), \quad (2.81)$$

where

$$E'(z) = H_0 \left[ \Omega_\Lambda - \frac{\Omega_m}{2} (1+z)^3 \right]. \quad (2.82)$$

For the Friedmann Cosmology ( $\Lambda = 0$ ), the substitution of  $1+z = a_0/a(t)$  into Eqs. 2.56 and 2.57 gives

$$E(z) = (1+z) \sqrt{1 + 2q_0 z}, \quad (2.83)$$

and

$$E'(z) = -q_0 (1+z)^3. \quad (2.84)$$

Eq. 2.83 had been commonly employed in the literature prior to acceptance of the  $\Lambda$  Cosmology.

The cosmological expansion rate per unit scale factor,  $\dot{a}(t)/a(t)$ , is illustrated in the left panel of Fig. 2.2 for three cosmological models. Denoting the models by  $(\Omega_m, \Omega_\Lambda)$ , the three cosmologies are the low-density (0.1,0) Einstein-de Sitter (1.0,0), and the  $\Lambda$  Cosmology (0.3,0.7). They are represented by the dotted, dashed, and solid curves, respectively. The low-density and Einstein-de Sitter models are subsets of the Friedmann cosmologies. The left axis gives the expansion rate as  $H(z)$ , the Hubble constant as measured by a hypothetical observer at redshift  $z$  for  $h = 0.7$ .

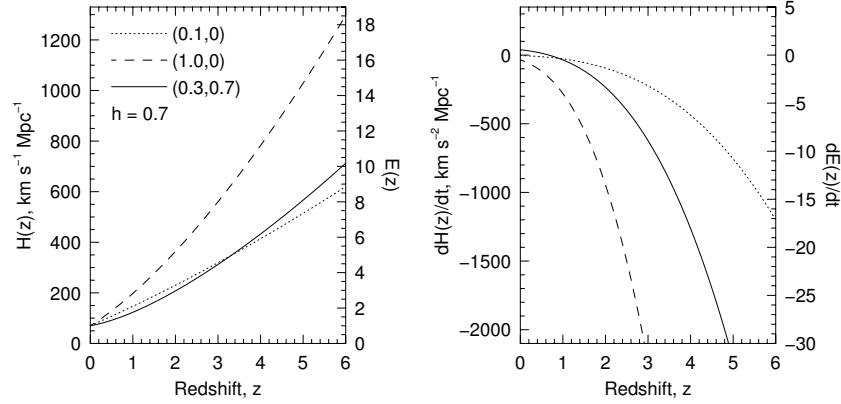


Figure 2.2: — (left) The cosmological expansion rate,  $\dot{a}/a$ , given by Eq. 2.79, versus redshift. Three cosmologies are shown, denoted by  $(\Omega_m, \Omega_\Lambda)$ ; (i) the low-density (0.1,0), dotted; (ii) Einstein-de Sitter (1.0,0), dashed; and the  $\Lambda$  Cosmology (0.3,0.7), solid. The left hand scale provides the expansion rate in Megaparsecs for  $h = 0.7$ . The right hand scale provides the expansion rate in units of  $H_0$ , which is the function  $E(z)$ . Note that  $\dot{a}/a = H_0$  and  $E(z) = 1$  at  $z = 0$ . — (right) The cosmological acceleration rate,  $\ddot{a}/a$ , given by Eq. 2.81, versus redshift for the same cosmologies. Note, the positive acceleration at low redshift in the  $\Lambda$  Cosmology.

The right axis gives the expansion rate normalized by  $H_0$ , which is the function  $E(z)$ , given by Eq. 2.80.

The cosmological acceleration rate per unit scale factor,  $\ddot{a}(t)/a(t)$ , is illustrated in the right panel of Fig. 2.2 for the three same cosmological models. Note  $\ddot{a}(t)/a(t) > 0$  in the  $\Lambda$  Cosmology at small  $z$ . The transition from deceleration to acceleration is obtained by nulling Eq. 2.81,

$$z = \left( \frac{2\Omega_\Lambda}{\Omega_m} \right)^{1/3} - 1, \quad (2.85)$$

which evaluates to  $z \simeq 0.6$  for the maximum likelihood cosmological parameters given in Eq. 2.71. At this redshift, the dark energy became the dominate energy density in the universe. The current (positive) acceleration rate per scale factor is a mild  $\simeq 40 \text{ km s}^{-2} \text{ Mpc}^{-1}$ .

### 2.6.1 Hubble's Law

Hubble's famous law provided the first definitive observational clue that the universe was expanding. By measuring both the redshifts and proper distances to galaxies, Hubble found that redshift and distance were linearly proportional. Today, two forms of Hubble's Law are tossed around, one

that is a linear relation between redshift and distance (Hubble's original finding), and one that is a relation between velocity and distance (obtained by equating redshift and velocity). Technically, the redshift–distance law is valid only for the local universe (i.e.,  $z \ll 1$ ). It can be derived by expanding the time evolution of the expansion factor near its present value,

$$a(t) = a_0 + \dot{a}_0(t - t_0) + \frac{1}{2}\ddot{a}_0(t - t_0)^2 + \dots \quad (2.86)$$

where  $t_0$  is the present time and  $t_0 > t$ . From the definition of Hubble's constant,  $H_0 = \dot{a}_0/a_0$ , and writing  $\Delta t = t_0 - t$ , the series can be rewritten

$$a(t)/a_0 = 1 - H_0\Delta t - \frac{1}{2}q_0H_0^2\Delta t^2 + \dots, \quad (2.87)$$

which provides the origin of the deceleration parameter, Eq. 2.55,

$$q_0 = -\frac{1}{H_0^2} \frac{\ddot{a}_0}{a_0} = -\frac{\ddot{a}_0 a_0}{\dot{a}_0^2}. \quad (2.88)$$

Since  $1 + z = a_0/a(t)$ , we have

$$1 + z = \frac{1}{[1 - H_0\Delta t - (q_0H_0^2/2)\Delta t^2 + \dots]} \approx 1 + H_0\Delta t, \quad (2.89)$$

which gives

$$z \simeq H_0\Delta t. \quad (2.90)$$

In the local universe,  $c\Delta t = l$  is the relation between the proper distance,  $l$ , to a object and the time for a light signal to travel to us. Substituting into Eq. 2.90, yields

$$cz = H_0l. \quad (2.91)$$

This is Hubble's original formulation based upon direct observations of  $z$  and  $l$  to galaxies.

The conversion to the velocity–distance Hubble Law, can be obtained from the relationship  $a_0/a(t) = \lambda/\lambda_r = 1 + z$ , we have

$$z = \frac{a_0 - a(t)}{a(t)} = \frac{\lambda - \lambda_r}{\lambda_r} = \frac{v}{c}, \quad (2.92)$$

where the right hand term follows from the Doppler effect for  $z \ll 1$ . We see that  $v = cz$ ; thus, for  $z \ll 1$ , we can measure recessional velocity directly from the spectroscopic redshift. We have

$$v = H_0l. \quad (2.93)$$

As we will discuss in § 2.9, this form of the law is technically valid for all redshifts if  $l$  is taken as the proper distance to the object and  $H_0$  is replaced with  $H(z)$ .

## 2.7 Time and Redshift

The time element,  $dt$ , and redshift element,  $dz$ , are equated through Eq. 2.65,

$$d\tau = cdt = dl_r = D_H \frac{da}{a(t)E(t)}, \quad (2.94)$$

which follows directly from  $ds = 0$  and  $d\psi = 0$  in the Robertson–Walker metric. and applying Eq. 2.77, i.e.,  $da/a(t) = dz/(1+z)$ . We have

$$dt = \frac{dl_r}{c} = \frac{1}{H_0} \frac{da}{a(t)E(t)} = \frac{1}{H_0} \frac{dz}{(1+z)E(z)} \quad (2.95)$$

The quantity  $t_H = 1/H_0$  is known as the Hubble Time

$$t_H = 9.78h^{-1} \text{ Gyr}, \quad (2.96)$$

which for  $h = 0.70$ , yields  $t_H = 14.0$  Gyr.

The time elapsed in the universe at an arbitrary redshift is simply the integral of the time element,  $dt$ , from redshift  $z$

$$t(z) = \int_z^\infty dt = t_H \int_z^\infty \frac{dz}{(1+z)E(z)}. \quad (2.97)$$

Substituting the lower limit of the integral with  $z = 0$  gives,  $t_0$ , the present age of the universe,

$$t_0 = t_H \int_0^\infty \frac{dz}{(1+z)E(z)}. \quad (2.98)$$

To determine the time elapsed since an event at redshift  $z$ , we compute the so-called “look-back time”, which is defined as  $t_{LB} = t_0 - t(z)$ , the difference between the present age of the universe and the age corresponding to when the photons were emitted (or absorbed). This quantity is simply given by the integral of the time element (Eq. 2.95) integrated over the redshift of the photon travel,

$$t_{LB} = t_H \int_0^z \frac{dz}{(1+z)E(z)}. \quad (2.99)$$

For a Friedmann Cosmology, Eq. 2.95 reduces to

$$dt = t_H \frac{dz}{(1+z)^2 \sqrt{1+2q_0z}}, \quad (2.100)$$

and the integrals in Eqs. 2.98 and 2.99 have analytic solutions  $t_0 = t_H$  ( $q_0 = 0$ ) and  $t_0 = 2t_H/3$  ( $q_0 = 0.5$ ) for the age of the universe. The look-back time is

$$t_{LB} = t_H [1 - (1+z)^{-1}] \quad (2.101)$$

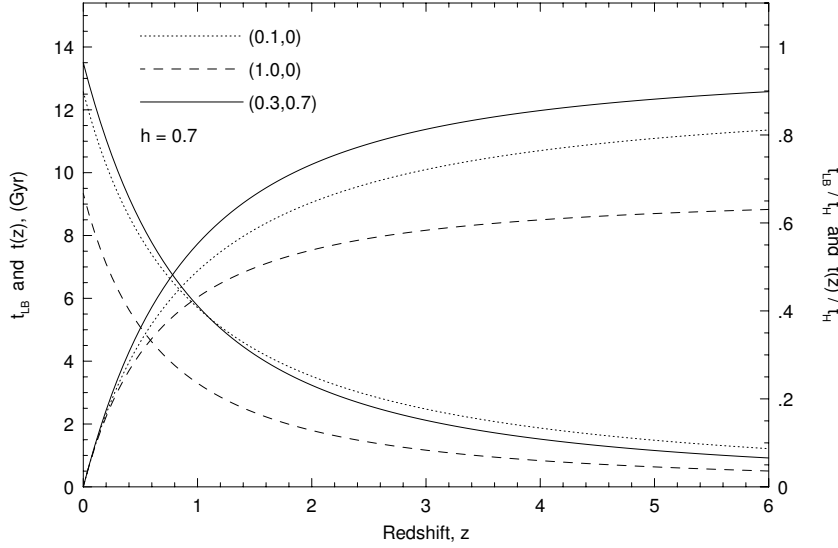


Figure 2.3: — The time elapsed at redshift  $z$ ,  $t(z)$ , and the look-back time,  $t_{LB}$ , versus redshift. The left axis gives the times in Gigayears for  $h = 0.7$ . The right axis gives the times in units of the Hubble Time,  $t_H$ . Three cosmologies are shown, denoted by  $(\Omega_m, \Omega_\Lambda)$ ; (i) the low-density (0.1,0), dotted; (ii) Einstein-de Sitter (1.0,0), dashed; and the  $\Lambda$  Cosmology (0.3,0.7), solid. For each cosmology, the point where the curves cross is the redshift at which the universe is half its age. [Adapted from Hogg (1999)].

for  $q_0 = 0$ , and

$$t_{LB} = \frac{2}{3}t_H \left[ 1 - (1+z)^{-3/2} \right] \quad (2.102)$$

for  $q_0 = 0.5$ , respectively. The best estimate for the age of the universe is estimated from the *WMAP* analysis to be

$$t_0 = 13.7 \pm 0.2 \text{ Gyr, (current best estimate).} \quad (2.103)$$

In Fig. 2.3, the quantities  $t(z)$  and  $t_{LB}$  are shown for the low-density, Einstein-de Sitter, and  $\Lambda$  Cosmologies for  $h = 0.7$ . At  $z = 0$ , the value of  $t(z)$  is the age of the universe, and is equivalent to Eq. 2.98. The redshift at which the universe is half its present age occurs where the curves intersect for each cosmology. For  $h = 0.7$ , these are approximately,  $t_{1/2} = 4.7$  Gyr at  $z = 0.59$  for Einstein-de Sitter Cosmology,  $t_{1/2} = 6.9$  Gyr at  $z = 0.80$  for  $\Lambda$  Cosmology, and  $t_{1/2} = 6.3$  Gyr at  $z = 0.85$  for low-density Cosmology.

### 2.7.1 Time Interval Dilation

The proper time interval between events occurring in the inertial frame of a cosmologically redshift object will not be equivalent in the inertial frame of an observer at the present time. This can be illustrated using a heuristic scenario of, for example, the proper time interval between photon pulses from a redshifted object.

For photons on radial trajectories, we set  $d\psi = 0$  and  $ds = 0$  in the Robertson–Walker metric, where the latter is due to the fact that photons travel on geodesics. Applied to the metric as expressed in Eq 2.61, we have

$$d\tau = cdt = dl_r = \frac{a(t)}{a_0} dD_c, \quad (2.104)$$

where  $dl_r = (a(t)/a_0)dD_c$  is the proper distance element a photon has traveled by the time the next pulse is emitted, i.e., the proper distance element between pulses. Let  $dt_e$  be the proper time element between pulses at the time of emission,  $t_e$ , from a redshifted emitting object. We have

$$dt_e = \frac{a(t_e)}{a_0} \frac{dD_c}{c}, \quad (2.105)$$

The observer measures the pulses at  $t = t_0$ , and the observed proper time element between pulses is

$$dt_0 = \frac{a(t_0)}{a_0} \frac{dD_c}{c} = \frac{D_c}{c}. \quad (2.106)$$

Taking the ratio, we have

$$\frac{dt_0}{dt_e} = \frac{a_0}{a(t_e)}, \quad (2.107)$$

which arises because the evolution of the scale factor has increased the the proper distance element between pulses at the observer by the factor  $a_0/a(t_e)$ .

Substituting  $1 + z = a_0/a(t_e)$ , we see that the proper time interval between events at the cosmologically redshifted emitter,  $\Delta t$ , is increased to a longer proper time interval,  $\Delta t_0$ , for an observer at the present time,

$$\Delta t_0 = (1 + z) \Delta t. \quad (2.108)$$

This time dilation is a real and observable consequence of the relativistic dynamics of the expansion of space and must be taken into account when measuring the time interval between events in the inertial frame of a cosmologically redshifted object.



## 2.8 Distance and Redshift

The characteristic distance of the universe is called the Hubble Distance, defined by

$$D_H = \frac{c}{H_0} = 3000h^{-1} \text{ Mpc}, \quad (2.109)$$

which gives  $D_H = 4283 \text{ Mpc}$  as the currently accepted value for  $h = 0.7$ . The Hubble Distance is a constant of proportionality for all cosmological distance measures.

There are multiple definitions for distances in the cosmological setting and they are primarily operational in nature, i.e., based upon the specific quantities being measured. This can lead to some confusion as to which distance measure is applicable in a given situation, and so some care must be taken to understand the connection between the observed quantity and the application of the appropriate distance measure. Some observations are radial (along a line of sight), while other observations involve a transverse component, i.e., the separation between two objects or an accounting of the angular extension of the object.

These “operational” definitions of distance derive from the Robertson–Walker metric, as outlined in § 2.3.3. Recall that the metric has both a proper radial element,  $dl_r$ , and a proper transverse element,  $dl_T$ . These are proportional to the radial co-moving element,  $dD_c$ , and the transverse co-moving element,  $D_T d\psi$ , respectively, where the proportionality is given by the time dependent scale factor  $a(t)/a_0$ . Below is a brief synopsis of the operational definitions of the various distance measures:

- *Proper Distance:* The radial proper distance,  $l$ , is the line of sight separation between two objects that share the same time coordinate. In the metric, these are obtained by setting  $dt = 0$  and  $d\psi = 0$ . The radial proper distance increases with time by the factor  $a(t)/a_0 = (1+z)^{-1}$ .
- *Co-moving Distance:* The radial co-moving distance,  $D_c$ , is a fixed quantity (no time dependence). It is the rigid coordinate distance in the absence of expansion. It is mathematically equivalent to the radial proper distance between two objects at the present time (i.e.,  $t = t_0$ ,  $z = 0$ ), when  $a(t)/a_0 = 1$ .
- *Transverse Co-moving Distance:* The transverse co-moving distance,  $D_T$ , is a non-radial distance to an object (basically the path length of the photon from object to observer). It is employed to compute the co-moving separation,  $S_c$ , between two objects separated by a fixed angle,  $\theta = \int d\psi$ , on the sky.

- *Proper Separation:* The proper separation,  $S$ , is the transverse proper distance between two objects that share the same time coordinate ( $dt = 0$  in the metric). It is obtained from the transverse proper distance element,  $dl_T d\psi$ , and is therefore proportional to both the transverse co-moving distance,  $D_T$  and the observed angle of separation,  $\theta$ , between the objects. The proper separation, like the radial proper separation, increases with time by the factor  $a(t)/a_0 = (1+z)^{-1}$ .
- *Angular Diameter Distance:* The angular diameter distance,  $D_A$ , is defined as the ratio of the proper separation,  $S$ , of two objects to the angular separation on the sky,  $\theta$ . It is utilized to compute the proper separation of two objects or the physical size of an extended object. It is also employed to compute the proper separation of two lines of sight as a function of redshift in gravitational lenses.
- *Absorption Distance:* The absorption distance is a modified redshift pathlength over which the probability of intersection in a line of sight survey is made constant for non-evolving objects. It normalizes out the evolution of the combined radial and transverse proper distances as a function of redshift.
- *Luminosity Distances:* Luminosity distance,  $D_L$ , is a distance based upon the observed flux of an object as compared to its luminosity. Discussion of this distance is reserved for § 2.12.1.

### 2.8.1 Radial Proper and Co-moving Distances

The radial proper distance element is defined by  $dt = 0$  in the Robertson–Walker metric (Eq. 2.15) with  $d\psi = 0$ . From the definition of the proper distance elements given in Eq. 2.63, we have

$$dl_r = \frac{a(t)}{a_0} dD_c = \frac{dD_c}{1+z}. \quad (2.110)$$

Integration gives the radial proper distance

$$l = \frac{D_c}{1+z}, \quad (2.111)$$

where  $D_c$  the radial co-moving distance derived in § 2.3.3,

$$D_c = a_0 D_H \int_{a_0}^{a(t_e)} \frac{da}{a^2(t)E(t)}. \quad (2.112)$$

Applying  $a_0/a(t) = 1 + z$  and  $da/a(t) = dz/(1 + z)$ , we have

$$D_c = D_H \int_0^z \frac{dz}{E(z)}, \quad (2.113)$$

where  $E(z)$  is given by Eq. 2.80 for the  $\Lambda$  Cosmology and Eq. 2.83 for the Friedmann Cosmology ( $\Lambda = 0$ ). For the Friedmann Cosmology, the integral can be evaluated analytically, yielding

$$D_c = D_H \left[ \frac{zq_0 + (q_0 - 1)(\sqrt{1 + 2q_0z} - 1)}{q_0^2(1 + z)} \right]. \quad (2.114)$$

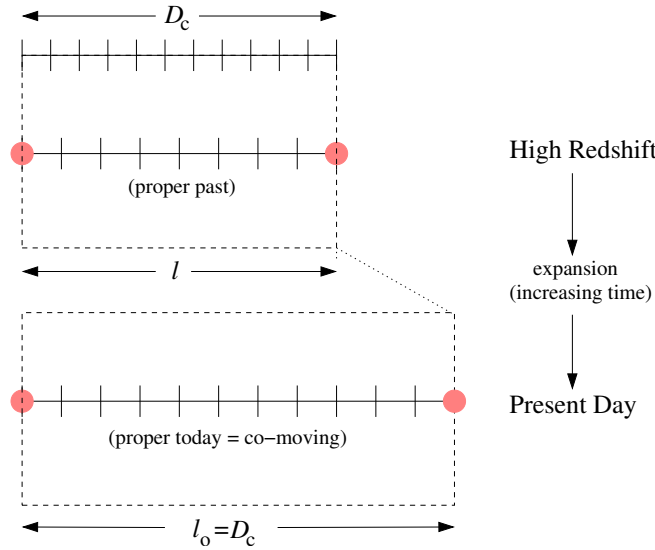


Figure 2.4: — A schematic of the meaning of co-moving distance. The proper distance,  $l$ , between two objects at a given redshift,  $z$ , will increase with decreasing redshift according to  $(a/a_0)l = l/(1 + z)$ , becoming  $l_0$  at the present time. In this example,  $l = 8\delta l$  intervals at  $z = 0.375$  have expanded to  $l_0 = 11\delta l$  intervals at the current epoch. We define the co-moving distance as the proper distance objects at higher  $z$  would have at the present time. This is a number fixed for all redshifts, as illustrated across the top of the high redshift panel. The co-moving distance normalizes out the cosmological expansion in order to place distance intervals on a common scale for all cosmic times.

A schematic of radial co-moving distance is given in Fig. 2.4. The upper panel represents the proper distance interval,  $l$ , between two objects in the past (higher redshift). Subsequent expansion increases the proper distance to  $l_0$  at the present time,  $t = t_0$ . Setting  $t = t_0$  gives  $a(t_0)/a_0 = 1$  and we have  $l_0 = D_c$ . Note that the scale for  $D_c$  along the top of the high redshift

panel has the same number of intervals as the proper distance at  $z = 0$ . The co-moving distance normalizes out the cosmological expansion and allows direct comparison of distance intervals at different epochs by standardizing them to the present epoch. This also introduces a physical interpretation of the co-moving coordinate,  $\chi$ , which “removes” the expansion of the universe. In co-moving coordinates, space is static, time does not dilate, objects carried by the Hubble flow are at rest with respect to one another, and photons have fixed wavelengths.

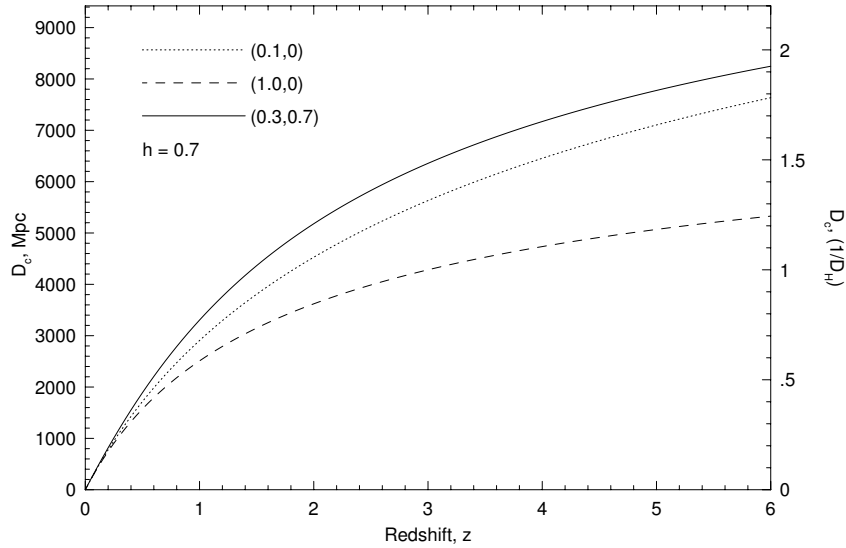


Figure 2.5: — The total radial co-moving distance, given by Eq. 2.113. Three cosmologies are shown, denoted by  $(\Omega_m, \Omega_\Lambda)$ ; (i) the low-density  $(0.1,0)$ , dotted; (ii) Einstein-de Sitter  $(1.0,0)$ , dashed; and the  $\Lambda$  Cosmology  $(0.3,0.7)$ , solid. The left hand scale provides the distance in Megaparsecs for  $h = 0.7$ . The right hand scale provides the distance in units of  $D_H$  [Adapted from Hogg (1999)].

The total radial co-moving distance,  $D_c$ , which is illustrated in Fig. 2.5 for the low-density, Einstein-de Sitter, and  $\Lambda$  Cosmologies, is a fundamental distance measure. The left axis of Fig. 2.5 gives  $D_c$  in Megaparsecs for  $h = 0.7$ . The right axis gives  $D_c/D_H$ , where  $D_H = 4283$  Mpc for  $h = 0.70$ .

### 2.8.1.1 Radial Separations

Consider an object at  $z = z_1$  and a second higher redshift object at  $z = z_2$ . The co-moving distance between the objects must properly account for the scale factor expansion from the epoch at  $z_2$  to the epoch at  $z_1$ . Defining

the expansion factor at  $z_2$  as  $a_2 = a(t_2)$  and the expansion factor at  $z_1$  as  $a_1 = a(t_1)$ , the relative expansion from  $z_2$  to  $z_1$  in the function  $E(t)$  (Eq. 2.46), appearing in the definition of the radial co-moving distance (Eq. 2.112), is now

$$E(t) = \left[ \Omega_m \left( \frac{a_1}{a_2} \right)^3 + \Omega_k \left( \frac{a_1}{a_2} \right)^2 + \Omega_\Lambda \right]^{1/2}, \quad (2.115)$$

where

$$\frac{(a_0/a_2)}{(a_0/a_1)} = \frac{1+z_2}{1+z_1} = \frac{a_1}{a_2} = 1+z_{12}. \quad (2.116)$$

Thus, the radial co-moving separation between two high redshift objects is mathematically equivalent to obtaining the total radial co-moving distance from  $z = 0$  to  $z = z_{12}$ , giving

$$D_c(z_1, z_2) = D_H \int_0^{z_{12}} \frac{dz}{E(z)}, \quad (2.117)$$

which is *not* equivalent to subtracting the total radial co-moving distance of the object at  $z_1$  from the total radial co-moving distance of the object at  $z_2$ . The radial proper separation is then  $l(z_1, z_2) = D_c(z_1, z_2)/(1+z_{12})$ .

### 2.8.2 Transverse Proper and Co-Moving Distances

As with the radial proper distance, the transverse distance element is defined by  $dt = 0$  in the Robertson–Walker metric (Eq. 2.15), but with  $d\psi \neq 0$ . The metric is  $ds = l_T d\psi$  for transverse separations. From the definition of the proper distance elements given in Eq. 2.62, we have

$$ds = l_T d\psi = \frac{a(t)}{a_0} \frac{D_H}{\sqrt{\Omega_k}} f_k(\chi) d\psi = \frac{a(t)}{a_0} D_T d\psi, \quad (2.118)$$

where  $D_T$  is the transverse co-moving distance, given by (Eq. 2.63)

$$D_T = \frac{D_H}{\sqrt{\Omega_k}} f_k(\chi), \quad (2.119)$$

where (Eq. 2.16),

$$f_k(\chi) = \begin{cases} \sin \chi & \text{positive} & \Omega_k < 0 \\ \chi & \text{flat} & \Omega_k = 0 \\ \sinh \chi & \text{negative} & \Omega_k > 0. \end{cases} \quad (2.120)$$

By comparing Eq. 2.68 and the definition of  $D_c$  in Eq. 2.112, we see that

$$\chi = \sqrt{\Omega_k} \frac{D_c}{D_H} \quad (2.121)$$

where  $D_c$  is the total radial co-moving distance, also given by Eq. 2.113 in terms of redshift.

Integrating over the angular element gives the transverse proper separation

$$S = l_T \int_0^\theta d\psi = \theta l_T = \frac{a(t)}{a_0} \theta D_T = \theta \frac{D_T}{1+z} \quad (2.122)$$

where  $\theta$  is directly observable from the sky separation of the two objects. As with the radial proper and co-moving distances, the transverse proper and co-moving separations are related by the scale factor,  $S = (a(t)/a_0)S_c$ , giving

$$S_c = \theta D_T. \quad (2.123)$$

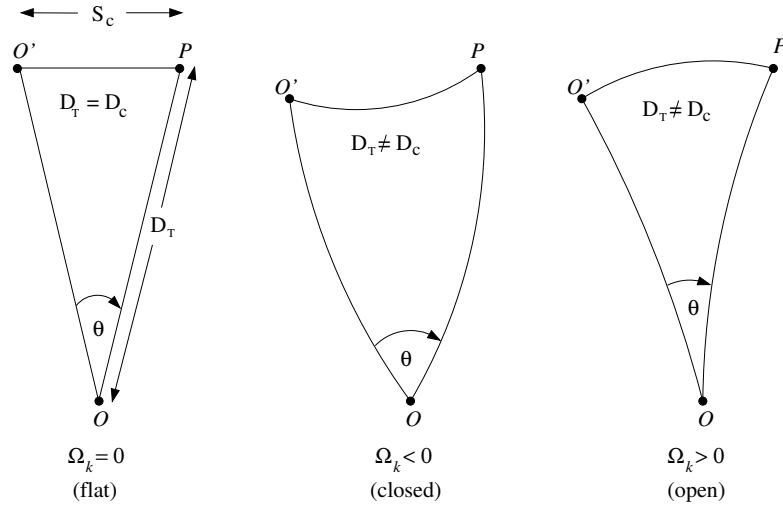


Figure 2.6: — The transverse co-moving distance,  $D_T$ , is used to compute the co-moving separation,  $S_c$ , between two objects,  $O'$  and  $P$ , at the same redshifts as observed at angular separation,  $\theta$ , by observer  $O$ . The observed angle  $\theta$  will depend upon the curvature of the universe. The functional form of  $D_T$  accounts for the curvature. [Adapted from Peebles (1993)].

Though the angle  $\theta$  is a direct observable, the measured angular separation is dependent upon the curvature of the universe, which dictates the angle of incident of the light path at the observer. As illustrated in Fig 2.6, consider an object  $P$  at redshift  $z$  as observed by observer  $O$  at  $z = 0$ . Consider a second object  $O'$  at the same redshift as object  $P$  separated by angle  $\theta$  as observed by  $O$ . The co-moving distance to  $P$  as observed by

observer  $O'$ , which is what we desire to measure, is the co-moving separation,  $S_c$ , as observed by  $O$ . This is the geometric configuration that gives the transverse co-moving distance its meaning; in a non-zero curvature geometry,  $D_T$  is not the radial co-moving distance— it is the path length of the photon traveling from an object that has angle of incidence  $\theta$  with respect to a photon traveling from another object (or location) at the same redshift.

Substituting  $\chi = \sqrt{\Omega_k}(D_c/D_H)$  into  $f_k(\chi)$ , for zero curvature,  $\Omega_k = 0$  (flat), we have

$$D_T = D_c \quad (\Omega_k = 0), \quad (2.124)$$

for positive curvature,  $\Omega_k < 0$  (closed), we have

$$D_T = \frac{D_H}{\sqrt{|\Omega_k|}} \sin \left( \sqrt{|\Omega_k|} \frac{D_c}{D_H} \right) \quad (\Omega_k < 0), \quad (2.125)$$

and for negative curvature,  $\Omega_k > 0$  (open), we have

$$D_T = \frac{D_H}{\sqrt{\Omega_k}} \sinh \left( \sqrt{\Omega_k} \frac{D_c}{D_H} \right) \quad (\Omega_k > 0). \quad (2.126)$$

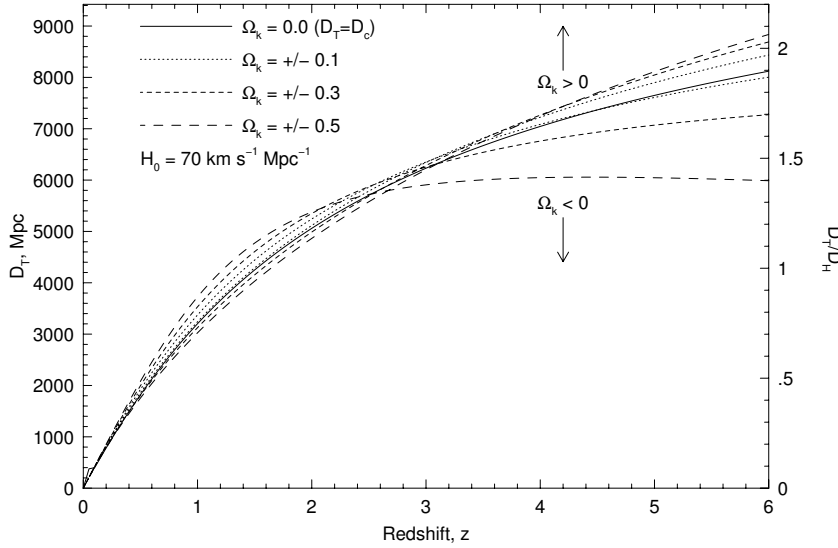


Figure 2.7: — The transverse co-moving distance, given by Eqs. 2.124–2.126, and 2.126. A  $\Lambda$  Cosmology is shown for  $\Omega_k = 0, \pm 0.1, \pm 0.2$ , and  $\pm 0.3$ , while enforcing  $\Omega_m = 0.3$ , and  $\Omega_m + \Omega_k + \Omega_\Lambda = 1$ .

In Fig. 2.7, an illustration of the behavior of the transverse co-moving distance is shown for various curvatures,  $\Omega_k = 0, \pm 0.1, \pm 0.2$ , and  $\pm 0.3$ . For this example, a  $\Lambda$  Cosmology is assumed with  $\Omega_m = 0.3$ , where Eq. 2.47 is enforced, i.e.,  $\Omega_m + \Omega_k + \Omega_\Lambda = 1$  (thus,  $\Omega_\Lambda$  varies). The right axis gives  $D_T/D_H$ , whereas the left axis is in Megaparsec for  $h = 0.7$ . The crossing of the curves is a result of enforcing Eq. 2.47, since varying  $\Omega_\Lambda$  changes the redshift for the onset of positive acceleration in the cosmological expansion.

Since  $\Omega_k = 0$  to good precision, Eq. 2.124 applies, and the co-moving separation between objects at the same redshift observed at a separation angle  $\theta$  is given by

$$S_c = \theta D_c, \quad (2.127)$$

which is the solid curve in Fig. 2.7.

### 2.8.2.1 Computing Angular Separation

Angular separation on the sky is computed as a difference between two measured positions on the sky. Positions are nominally measured in the ecliptic coordinate system using right ascension (RA, denote  $\alpha$ , increasing from west to east) and declination (DEC, denoted  $\delta$ , positive north, negative south, increasing in magnitude toward the poles).

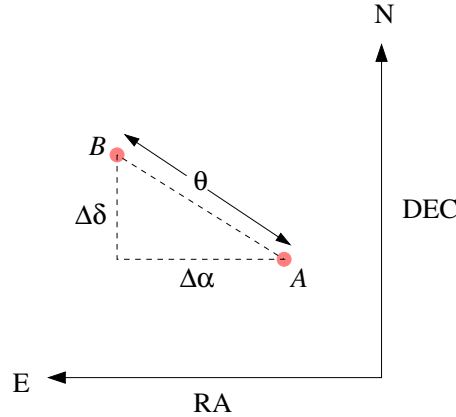


Figure 2.8: — Schematic for measuring angular separation,  $\theta$ , on the sky for two objects  $A$  and  $B$  in the ecliptic coordinate system, right ascension and declination. North is upward and east is to the left. The proper formula to compute  $\theta$  from  $\Delta\alpha$  and  $\Delta\delta$  is given by Eq. 2.130

As illustrated in Fig. 2.8, if position  $A$  is located at  $\alpha_1$  and  $\delta_1$  and position  $B$  is located at  $\alpha_2$  and  $\delta_2$ , then the angular separation in each



coordinate is

$$\Delta\alpha = \alpha_2 - \alpha_1 \quad (2.128)$$

$$\Delta\delta = \delta_2 - \delta_1, \quad (2.129)$$

where care must be taken if the two  $\alpha$  are on opposite sides of the celestial prime meridian or if the two  $\delta$  are on opposite sides of the celestial equator (it is a good idea to convert to radians before performing the above operation).

The angular separation,  $\theta$ , in these two sky locations is *not* simply the quadrature sum,  $\sqrt{\Delta\alpha^2 + \Delta\delta^2}$ . At the celestial equator the quadrature sum is exact, but for non-zero  $\delta$ , the geometric projection on the surface of the celestial sphere must be taken into account. The proper formula to compute angular separation of object  $B$  from object  $A$  on the sky is

$$\theta = \sqrt{(\Delta\alpha)^2 \cos^2 \delta_1 + (\Delta\delta)^2} \quad (2.130)$$

### 2.8.3 Angular Diameter Distance

The angular diameter distance,  $D_A$ , is technically not a distance. It is formally defined as the ratio of the transverse proper separation,  $S$ , to the angular separation,  $\theta$ . From Eqs. 2.122 and 2.123,

$$S = \frac{S_c}{1+z} = \frac{\theta D_T}{1+z}. \quad (2.131)$$

By definition, the angular diameter distance is  $S/\theta$ , which gives

$$D_A \equiv \frac{S}{\theta} = \frac{D_T}{1+z}. \quad (2.132)$$

Rewriting 2.131, gives

$$S = \theta D_A. \quad (2.133)$$

Similarly, the physical transverse size of an object with angular size  $\theta$  is also computed from Eq. 2.131. Expressing the transverse proper separation in terms of angular separations measured in arcseconds yields,

$$S = \theta D_A = \frac{14.54 h^{-1}}{1+z} \left( \frac{\theta}{1''} \right) \left( \frac{D_T}{D_H} \right) \text{ kpc}. \quad (2.134)$$

The angular diameter distance,  $D_A$ , given in units  $h^{-1}$  kiloparsecs per arcsec of angular separation, is shown in Fig. 2.9 for the low-density, Einstein-de Sitter, and  $\Lambda$  Cosmologies. A rule of thumb is that two objects at  $z \simeq 1$  separated by  $1''$  have a physical separation of  $\simeq 5 h^{-1} \text{ kpc}$ .

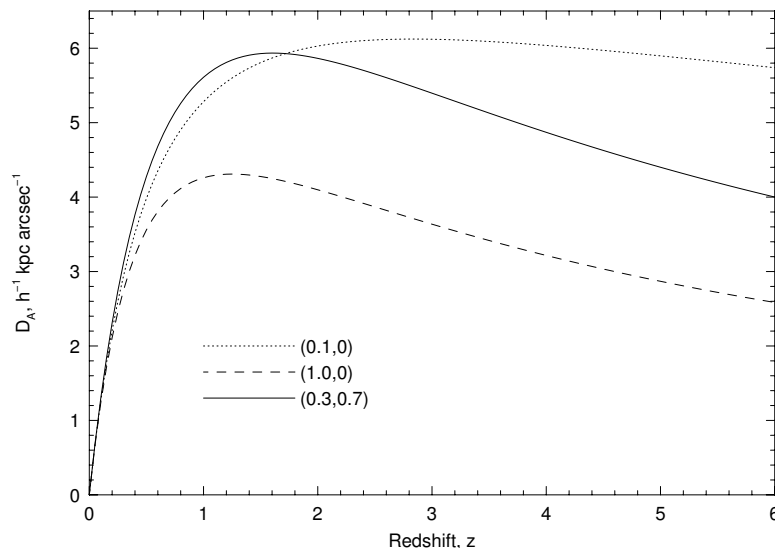


Figure 2.9: The angular diameter distance,  $D_A$ , between two objects at the same redshift given in the units  $h^{-1} \text{ kpc arcsec}^{-1}$ , as given by Eq. 2.134. Three cosmologies are shown, denoted by  $(\Omega_m, \Omega_\Lambda)$ ; (i) the low-density (0.1,0), dotted; (ii) Einstein-de Sitter (1.0,0), dashed; and the  $\Lambda$  Cosmology (0.3,0.7), solid.

Note that  $D_A$  maximizes for  $z \sim 1$ , and then decreases for higher redshifts. Take note that  $\Omega_k = 0$  for both the Einstein-de Sitter and  $\Lambda$  Cosmologies, so that  $D_T = D_c$  in Eq. 2.134. However, for the low-density case,  $\Omega_k = 1 - \Omega_m = 0.9$ , so that  $D_T$  must be computed from Eq. 2.126.

In the application of quasar absorption lines, if the absorbing gas is associated with galaxies, then the projected galactocentric distance of the quasar line of sight to the galaxy, i.e., the impact parameter, can be computed from  $\theta$  and Eq. 2.134. A second application is quasar pairs (not gravitational lenses) having close proximity on the sky. In this case the line of sight separation at a given redshift is also given by Eq. 2.134.

### 2.8.4 Proper Separations in Lenses

In gravitational lens, multiple images of the light source will be seen. Thus, there will be multiple lines of sight that can be observed simultaneously. For the majority of the time that the light travels, the paths follow the curvature of universe. However, in the proximity of the lens, the paths are deflected by the local curvature induced by the lensing mass. In cosmological applications, the pathlength of the deflection is negligible. Thus, to a

good approximation, the deflection can be treated as instantaneous; that is, the light paths can be treated as following the curvature of the universe from source to lens and then, post deflection, from lens to observer.

A schematic of the geometry of a lens system is shown in Eq. 2.10, where the observer  $O$  is at  $z = 0$ , the lens  $l$  is at  $z = z_l$ , and the source  $Q$  is at  $z = z_s$ . The observer measures the two images,  $A$  and  $B$ , to have angular separation  $\theta$ . Consider some arbitrary redshift,  $z_c$ , where absorption arises from a single non-rotating gas cloud probed by the both lines of sight. We wish to compute the proper separation,  $S(z_c)$ , of the lines of sight for all redshifts  $0 \leq z_c \leq z_s$ .

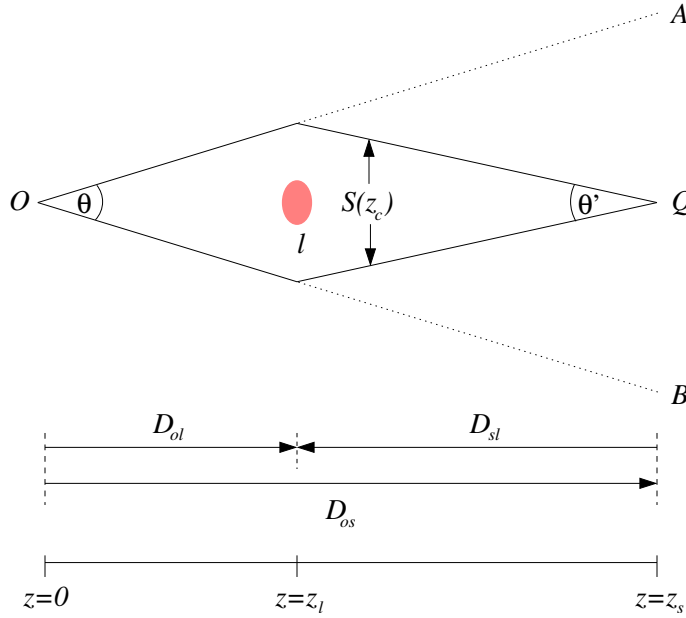


Figure 2.10: — A schematic of gravitational lens geometry and the quantities involved in the computation of  $S(z_c)$ , the proper separation of the two lines of sight,  $A$  and  $B$ , at arbitrary redshift  $z_c$ . To the observer,  $O$ , the lines of sight have angular separation  $\theta$  and the source  $S$ , is seen as the two images  $A$  and  $B$ ; to the source, the lines of sight have angular separation  $\theta'$ . [Adapted from Smette et al. (1992)].

For  $z_c \leq z_l$ , the proper separation of the light paths is

$$S(z_c) = \theta D_{oc}(z_c) \quad (z_c \leq z_l), \quad (2.135)$$

where  $D_{oc}$  is the angular diameter distance from the observer to the cloud (this result is identical to Eq. 2.133).

To obtain the proper separation for  $z_c > z_l$ , consider the light paths from the view point of the source,  $Q$ . The proper separation of the light paths is

$$S(z_c) = \theta' D_{sc}(z_c), \quad (2.136)$$

where  $\theta'$  is the separation angle of the light paths from  $Q$ , and  $D_{sc}$  is the angular diameter distance from the source to the cloud (yes, oriented from high redshift to low redshift!). Since we cannot measure  $\theta'$ , we need to obtain the geometric relationship between  $\theta'$  and  $\theta$ . From  $Q$ , the angular diameter distance to the lens is  $D_{sl}$  (notice the direction of the arrow denoting  $D_{sl}$  in Fig 2.10) and the proper separation of the light paths at the lens is

$$S(z_l) = \theta' D_{sl}. \quad (2.137)$$

From  $O$ , the proper separation of the light paths at the lens is

$$S(z_l) = \theta D_{ol}, \quad (2.138)$$

where  $D_{ol}$  is the angular diameter distance to the lens from  $O$ . Equating Eqs. 2.138 and 2.137, yields the geometric relationship,

$$\theta' = \theta \frac{D_{ol}}{D_{sl}}. \quad (2.139)$$

Substituting Eq. 2.139 into Eq. 2.136, we have the proper separation of the light paths for  $z_c \geq z_l$ ,

$$S(z_c) = \theta \frac{D_{ol}}{D_{sl}} D_{sc}(z_c) \quad (z_c \geq z_l), \quad (2.140)$$

which is known as the lens equation. Together, Eqs. 2.135 and 2.140 describe the proper separation of the lines of sight from observer to source. For  $z_c \simeq z_l$ , there is some uncertainty due to the treatment of instantaneous deflection, which will be sensitive to the mass distribution.

In § 2.8.3, it was shown that the angular diameter distance from the observer to redshift  $z$  is computed from Eq. 2.132, i.e.,

$$D_{oz} = \frac{D_T(z)}{1+z}, \quad (2.141)$$

where  $D_T(z)$  is the transverse co-moving distance to redshift  $z$  (Eqs. 2.124, 2.125, or 2.126, depending upon the sign of  $\Omega_k$ ). However, in the lens equation, Eq. 2.140, angular diameter distances appear that are measured from  $z_s$  to  $z_l$  and from  $z_s$  to  $z_c$ .

In general, the angular diameter distance at redshift  $z_2$  as observed from redshift  $z_1$ , where  $z_2 > z_1$ , is

$$D_{12} = \frac{D_2 Q_1 - D_1 Q_2}{1 + z_2}, \quad (2.142)$$

where

$$\begin{aligned} Q_1 &= \left(1 + \Omega_k \frac{D_1^2}{D_H^2}\right)^{1/2} \\ Q_2 &= \left(1 + \Omega_k \frac{D_2^2}{D_H^2}\right)^{1/2} \end{aligned} \quad (2.143)$$

are the curvature terms, and where

$$D_1 = D_T(z_1) \quad D_2 = D_T(z_2). \quad (2.144)$$

In the lens equation, two of the terms,  $D_{sl}$  and  $D_{sc}(z_c)$ , are the angular diameter distance as observed *from* the source,  $Q$ , which is the higher redshift perspective. The inverse relationship to Eq. 2.142 is

$$D_{21} = \left(\frac{1 + z_2}{1 + z_1}\right) D_{12} = \frac{D_2 Q_1 - D_1 Q_2}{1 + z_1}. \quad (2.145)$$

It is important to apply the inverse relationship for the terms  $D_{sl}$  and  $D_{sc}(z_c)$  in the lens equation, or the separation will be overestimated.

For a Friedmann Cosmology ( $\Lambda = 0$ ), the analytic form is

$$D_{12} = 2D_H \left[ \frac{(1 - 2q_0)(Q_1 - Q_2) + (Q_1 Q_2^2 - Q_1^2 Q_2)}{(2q_0)^2(1 + z_1)(1 + z_2)^2} \right], \quad (2.146)$$

where the curvature terms reduce to

$$\begin{aligned} Q_1 &= \sqrt{1 + 2q_0 z_1} \\ Q_2 &= \sqrt{1 + 2q_0 z_2}. \end{aligned} \quad (2.147)$$

The inverse relationship of Eq. 2.145 also applies for Eq. 2.146.

#### 2.8.4.1 Zero Curvature Solution

Since  $\Omega_k = 0$  to good precision, the angular diameter distances (Eq. 2.142) appearing in the lens equation can be highly simplified. The curvature terms, Eq. 2.143, simplify to  $Q_1 = Q_2 = 1$ . Also, the transverse co-moving distance,  $D_T(z)$ , reduces to the radial co-moving distance,  $D_c(z)$ , as given by Eq. 2.124.

We have

$$D_{oc}(z_c) = \frac{D_c(z_c)}{1 + z_c} \quad (z_c < z_l), \quad (2.148)$$

for the light paths on the observer side of the lens, appearing in Eq. 2.135. For the source side of the lens, the terms in the lens equation, Eq. 2.140, reduce to

$$\begin{aligned} D_{ol} &= \frac{D_c(z_l)}{1 + z_l} \\ D_{sl} &= \frac{D_c(z_s) - D_c(z_l)}{1 + z_l} \\ D_{sc}(z_c) &= \frac{D_c(z_s) - D_c(z_c)}{1 + z_c} \end{aligned} \quad (2.149)$$

where the inverse relationship to Eq. 2.142 has been applied for  $D_{sl}$  and  $D_{sc}(z_c)$ , and where the radial co-moving distances are given by Eq. 2.113. For a Friedmann Cosmology ( $\Lambda = 0$ ), the co-moving distances are obtained from Eq. 2.114, from which Eq. 2.146 can be derived.

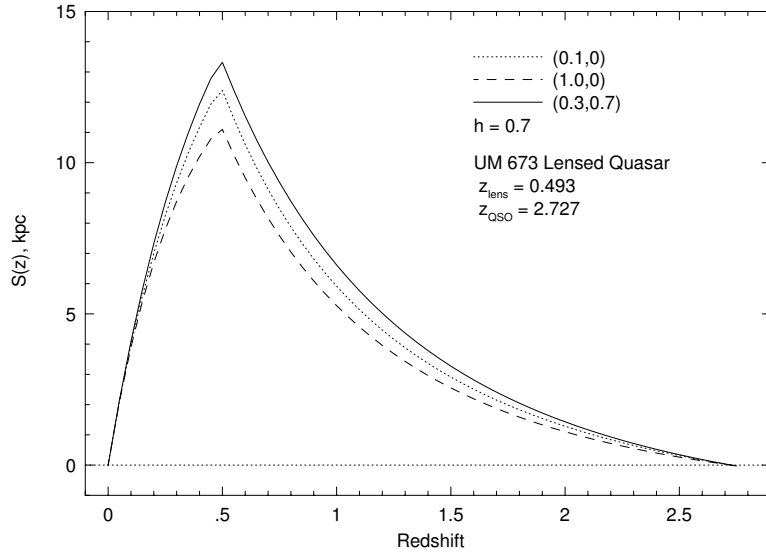


Figure 2.11: — The co-moving line of sight separation,  $S(z)$ , as a function of redshift for the UM 673 lensed quasar for  $h = 0.7$ . The quasar is at  $z_s = 2.727$ , and the lens is at  $z_l = 0.493$ . Three cosmologies are shown, denoted by  $(\Omega_m, \Omega_\Lambda)$ ; (i) the low-density (0.1,0), dotted; (ii) Einstein-de Sitter (1.0,0), dashed; and the  $\Lambda$  Cosmology (0.3,0.7), solid. [Adapted from Smette et al. (1992)].

In Fig. 2.11, the proper separation,  $S(z)$ , of the light paths for images  $A$  and  $B$  of the lensed quasar UM 673 are plotted for the low-density, Einstein-de Sitter, and  $\Lambda$  Cosmologies for  $h = 0.7$ . The lens parameters are  $z_s = 2.727$ ,  $z_l = 0.493$ , and  $\theta = 2.22''$  (Smette et al., 1992). For both the Einstein-de Sitter and  $\Lambda$  Cosmologies,  $\Omega_k = 0$  so that  $D_T = D_c$  and the curvature terms are unity. For these cases,  $S(z)$  was computed using Eq. 2.148 inserted into Eq. 2.135 and Eq. 2.149 inserted into Eq. 2.140. However, for the low-density case,  $\Omega_k = 1 - \Omega_m = 0.9$ , so that  $D_T$  must be computed from Eq. 2.126 and the curvature terms must be included in the computation of  $S(z)$ . Thus, the full formal treatment was used to compute  $S(z)$  for the low-density case. The  $q_0 = 0$  (0.1,0) and  $q_0 = 1/2$  (1.0,0) curves match the Smette et al. results (computed using Eq. 2.146 scaled to  $h = 0.5$ ).

## 2.9 Velocity and Redshift

Having defined the connections between redshift and time and also various distances, it is of interest to consider the concept of velocity, which is derived from the ratio of proper distance over travel time. The proper distance is

$$l = \frac{a(t)}{a_0} D_c = \frac{D_c}{1+z}, \quad (2.150)$$

where the co-moving distance is given by Eq. 2.113. Velocity is the time derivative of the proper distance,

$$v = \frac{dl}{dt} = \frac{\dot{a}(t)}{a_0} D_c + \frac{a(t)}{a_0} \dot{D}_c. \quad (2.151)$$

Writing  $v = v_{rec} + v_{pec}$ , we have the definitions of the cosmological velocity of recession (due to Hubble flow) and the so-called peculiar velocity,

$$\begin{aligned} v_{rec} &= \frac{\dot{a}(t)}{a_0} D_c \\ v_{pec} &= \frac{a(t)}{a_0} \dot{D}_c. \end{aligned} \quad (2.152)$$

The observed velocity of recession is dependent upon the expansion velocity at the epoch of the observation,  $\dot{a}(t)$ , where the observer is not necessarily in the inertial frame of the object. The peculiar velocity of an object, on the other hand, has meaning only when the observer and object, are in the same inertial frame (share the same time coordinate, i.e.,  $dt = 0$ )

in the metric). Similarly, for the peculiar velocity difference of two objects, the two objects must be in the same frame.  $\dot{D}_c$  can be interpreted as the velocity in co-moving coordinates (independent of expansion).

### 2.9.1 Peculiar Velocities

The peculiar velocity is defined in the local inertial frame of the observer. Thus, measured velocities obey the rules of Special Relativity; the peculiar velocity of a photon is always  $c$  and no object can have a velocity exceeding the speed of light.

The peculiar velocity of a photon can be derived from the definition of  $v_{pec}$  and the fact that photons travel on geodesics,  $ds = 0$ . Rewriting  $\dot{D}_c = dD_c/dt$ , we have

$$v_{pec} = \frac{a(t)}{a_0} \frac{dD_c}{dt} = \frac{a(t)}{a_0} \frac{dD_c}{d\chi} \frac{d\chi}{da} \frac{da}{dt} = c \quad (2.153)$$

which is obtained by substitution of Eqs. 2.64, 2.67, and 2.65, respectively.

Peculiar velocities of objects are induced by mechanical and dynamical interactions of structures local to one another, and are viewed as velocities that depart from the cosmological velocity of recession (i.e., the Hubble flow). Consider an object carried by the Hubble flow with redshift  $z$ , and a second “close-by” object at  $z$  that has a non-zero velocity with respect to the first object. When  $v_{pec} \ll c$ , the peculiar velocity induces a small redshift difference between the objects

$$\frac{\Delta z}{1+z} = \frac{v_{pec}}{c}, \quad (2.154)$$

where  $\Delta z = z_{obs} - z$ , and where  $z_{obs}$  will be the observed redshift of the object having the peculiar velocity, and  $z$  is the redshift for an object locked into the Hubble flow.

For larger velocities, the relationship  $v = cz$  breaks down. Accounting for special relativistic effects, redshift is related to velocity by

$$1+z = \sqrt{\frac{1+\beta}{1-\beta}}, \quad (2.155)$$

where  $\beta = v_{pec}/c$ . This is based upon the principle of the Doppler shift. Applying the relativistic formula for large redshift objects, we would assign an apparent velocity of

$$\beta = \frac{(1+z)^2 - 1}{(1+z)^2 + 1} \quad (2.156)$$



to an object at redshift  $z$ , and a velocity difference of

$$\beta_{12} = \frac{(1+z_2)^2 - (1+z_1)^2}{(1+z_2)^2 + (1+z_1)^2} \quad (2.157)$$

between objects at  $z_1$  and  $z_2$ , where  $z_2 > z_1$ .

It should remain appreciated that cosmological velocity of recession (also measured using redshift) is not an inertial frame measurement and thus does not obey the rules of Special Relativity. To apply Eq. 2.156 as a means of determining a velocity of recession to a cosmological object or Eq. 2.157 for the velocity of recession between objects is flat out incorrect. Thus, the applications of Eq. 2.156 has physical meaning only for objects that are both in the same inertial reference frame (relatively local to one another, or assumed to be).

### 2.9.2 Velocities of Recession

Recession velocities are not interpreted as a Doppler shift. Yet, a consequence of the expanding universe paradigm is that redshift is directly related to recessional velocity (Harrison, 1993). However, there has been confusion over the interpretation of this velocity because of the notion that no objects can recede at faster than light speed. Actually, it is a well documented misconception that the velocities of objects carried by the Hubble flow cannot exceed the speed of light (see Davis & Lineweaver, 2004). In the expanding universe formalism, there is no global reference frame. It is General Relativity and not Special Relativity that is employed for computing cosmological quantities. In General Relativity, motions outside the observer's inertial reference frame can be properly treated and are fully consistent with faster than light speed motion.

From Eq. 2.152, we have

$$v_{rec} = \frac{\dot{a}(t)}{a_0} D_c. \quad (2.158)$$

Rearranging  $\dot{a}(t)/a_0$  gives

$$\frac{\dot{a}(t)}{a_0} = \frac{\dot{a}(t)}{a(t)} \frac{a(t)}{a_0} = \frac{H_0 E(z)}{1+z}, \quad (2.159)$$

where  $E(z)$  is given by Eq. 2.80. The velocity of recession is then

$$v_{rec} = c \frac{E(z_o)}{1+z_o} \int_0^{z_e} \frac{dz}{E(z)}, \quad (2.160)$$

where  $c = H_0 D_H$  has been carried through from the definition of  $D_c$  (Eq. 2.113), and where  $z_o$  is the redshift (time) at which the photons are observed and  $z_e$  is the redshift (time) at which the photons were emitted. The proportionality factor,  $E(z_o)/(1 + z_o)$ , accounts for the fact that the recessional velocity of a co-moving object depends upon the epoch of observation, which occurs because the expansion rate is not constant with time. Recessional velocities “observed” at the present time are obtained by setting  $z_o = 0$ .

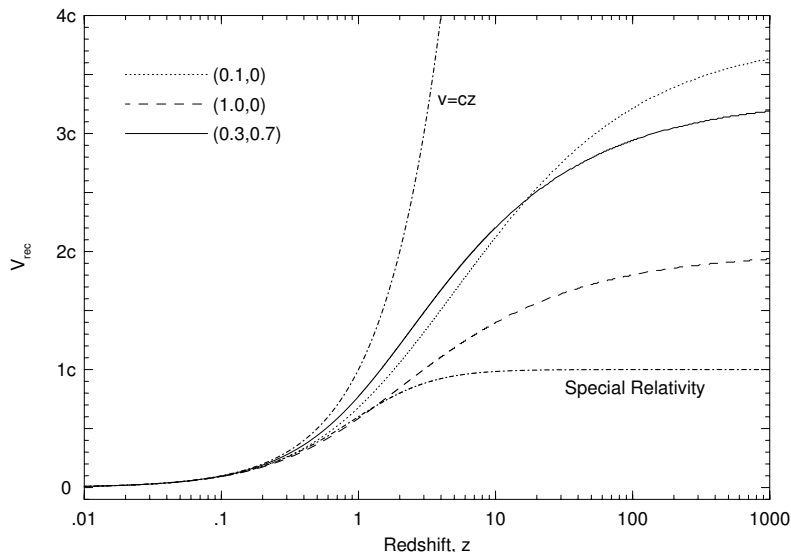


Figure 2.12: — The present day ( $z_o = 0$ ) velocity of recession for objects carried by the Hubble flow as a function of redshift. Three cosmologies are shown, denoted by  $(\Omega_m, \Omega_\Lambda)$ ; (i) the low-density (0.1,0), dotted; (ii) Einstein-de Sitter (1.0,0), dashed; and the  $\Lambda$  Cosmology (0.3,0.7), solid. The special relativity case (Eq. 2.156) and the linear relation,  $v = cz$ , are shown as thick dash-dot curves. For the  $\Lambda$  Cosmology, the recession velocity of objects exceeds the speed of light at  $z = 1.46$  [Adapted from Davis & Lineweaver (2004)].

In Fig 2.12, the recession velocity of cosmological objects is shown as a function of redshift as “observed” at the present time. The low-density, Einstein-de Sitter, and  $\Lambda$  Cosmologies are illustrated, as are the special relativity velocity law (Eq. 2.156) and the linear velocity law,  $v = cz$ . For  $z < 0.15$ , the various recession velocities are consistent. The recession velocity exceeds the speed of light for  $z = 1.46$  for the  $\Lambda$  Cosmology. Independent of cosmology, the onset of greater than light speed recession occurs at the Hubble Distance (see Fig 2.5 for the redshifts at which  $D_c/D_H = 1$ ). The region surrounding an observer at which the recession velocity of objects

exceeds the speed of light is called the Hubble sphere

$$D_{\text{HS}}(z) = c \frac{a(t)}{\dot{a}(t)} = \frac{c}{H(z)} = \frac{D_{\text{H}}}{E(z)}, \quad (2.161)$$

which grows with time (decreasing redshift).

Naively, it might be expected that the Hubble sphere is a horizon beyond which objects could not be observed because the photons propagating in our direction are being carried further away by the Hubble flow (i.e., they are receding!). In an expanding spacetime, the slope of our past light cone is not a constant, but is  $v_{\text{rec}} - c$ . So it is true; light emitted outside the Hubble sphere begins its journey receding from us (in proper distance). However, the size of the Hubble sphere evolves, receding from us with time. It can be visualized that for  $\dot{D}_{\text{HS}} = c[1 - a(t)/\ddot{a}^2(t)] > v_{\text{rec}} - c$ , the Hubble sphere will catch up to and “overtake” the receding photons. Light inside the Hubble sphere now a peculiar velocity of approach greater than the recession velocity (Hubble flow) and can eventually reach us as observers. The objects that emitted the light however, remain outside the Hubble sphere; they continue to recede at greater than light speed. For details, including spacetime diagrams illustrating the points made here, see Davis & Lineweaver (2004).

## 2.10 Volume and Redshift

The proper volume element is the product of the proper area element,  $dA$ , observed over solid angle  $d\Omega$  and the proper distance element,  $dl$ ,

$$dV = dA dl. \quad (2.162)$$

The proper area is

$$dA = D_{\text{A}}^2 d\Omega, \quad (2.163)$$

where  $D_{\text{A}}$  is the angular diameter distance (Eq. 2.132). The expression for  $dA$  follows from the same principle as the linear proper separations given by Eq. 2.133. The proper distance element is given by Eq. 2.95,

$$dl = c dt = D_{\text{H}} \frac{dz}{(1+z)E(z)}. \quad (2.164)$$

Written out, the proper volume element is

$$dV = D_{\text{H}} \frac{D_{\text{A}}^2}{(1+z)E(z)} d\Omega dz. \quad (2.165)$$

At the current epoch ( $z = 0$ ), the proper volume element per unit solid angle is

$$\frac{dV_0}{d\Omega} = D_{\text{H}} D_{\text{A}}^2. \quad (2.166)$$

More commonly applied in cosmological studies is the co-moving volume,  $V_c$ . In a co-moving volume, the number density of non-evolving objects remains constant as the universe expands. The co-moving volume element,  $dV_c$ , is the product of the co-moving area element,  $dA_c$ , observed over solid angle  $d\Omega$  and the radial co-moving distance element,  $dD_c$ ,

$$dV_c = dA_c dD_c. \quad (2.167)$$

The co-moving area element is

$$dA_c = D_{\text{T}}^2 d\Omega = (1+z)^2 D_{\text{A}}^2 d\Omega, \quad (2.168)$$

where  $D_{\text{T}}$  is the transverse co-moving distance (Eq. 2.123) and the right hand term follows from the definition of the angular diameter distance (Eq. 2.132). Written out, the co-moving volume element is

$$dV_c = D_{\text{H}} \frac{D_{\text{A}}^2 (1+z)^2}{E(z)} d\Omega dz. \quad (2.169)$$

Note that  $dV_c = (1+z)^3 dV$ , as might be intuitively expected.

The co-moving volume elements, Eq. 2.169 is shown in Fig. 2.13 for the low-density, Einstein-de Sitter, and  $\Lambda$  Cosmologies. The right hand axis provides the scale in units of the  $D_{\text{H}}^3$ , which is often called the Hubble Volume. The left hand axis provides the scale in  $10^9 \text{ Mpc}^3$  for  $h = 0.7$ . Note that the co-volume element is very sensitive to the cosmological parameters.

The integrated co-moving volume to redshift  $z$  is

$$V_c = D_{\text{H}} \int d\Omega \int_0^z \frac{D_{\text{A}}^2 (1+z)^2}{E(z)} dz. \quad (2.170)$$

If the volume is obtained using ecliptic coordinates, where  $\alpha$  is the right ascension and  $\delta$  is the declination, then

$$\Theta^2 = \int d\Omega = \int_{\alpha_1}^{\alpha_2} \int_{\delta_1}^{\delta_2} \sin \delta d\delta d\alpha, \quad (2.171)$$

where in principle  $\delta$  could be written as a function of  $\alpha$ . Performing the

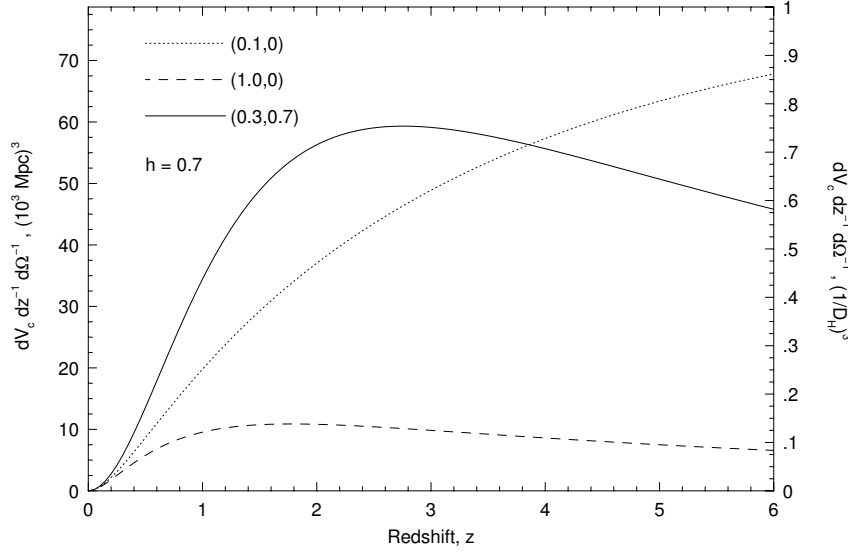


Figure 2.13: — The co-moving volume element per unit redshift per unit solid angle, given by Eq. 2.169. Three cosmologies are shown, denoted by  $(\Omega_m, \Omega_\Lambda)$ ; (i) the low-density (0.1,0), dotted; (ii) Einstein-de Sitter (1.0,0), dashed; and the  $\Lambda$  Cosmology (0.3,0.7), solid. The left hand scale provides the volume in cubic Megaparsecs ( $\times 10^9$ ) for  $h = 0.7$ . The right hand scale provides the distance in units of  $D_H$  [Adapted from Hogg (1999)]. Take note that  $\Omega_k = 0$  for both the Einstein-de Sitter and  $\Lambda$  Cosmologies, so that  $D_\Lambda = (1+z)D_c$ . However, for the low-density case,  $\Omega_k = 1 - \Omega_m = 0.9$ , so that  $D_z = (1+z)D_T$ , which must be computed from Eq. 2.126.

integration of Eq. 2.170 (see Carrol, Press, & Turner, 1992) gives

$$\begin{aligned}
 V_c &= \frac{\Theta^2}{3} D_c^3 & (\Omega_k = 0) \\
 V_c &= \frac{\Theta^2 D_H^3}{2\Omega_k} \left[ \frac{D_T}{D_H} Q - Y^+ \right] & (\Omega_k > 0) \\
 V_c &= \frac{\Theta^2 D_H^3}{2\Omega_k} \left[ \frac{D_T}{D_H} Q - Y^- \right] & (\Omega_k < 0),
 \end{aligned} \tag{2.172}$$

where

$$Q = \sqrt{1 + \Omega_k \frac{D_T}{D_H}} \tag{2.173}$$

and

$$\begin{aligned} Y^+ &= \frac{1}{\sqrt{\Omega_k}} \sinh^{-1} \left( \sqrt{\Omega_k} \frac{D_T}{D_H} \right) \\ Y^- &= \frac{1}{\sqrt{|\Omega_k|}} \sin^{-1} \left( \sqrt{|\Omega_k|} \frac{D_T}{D_H} \right). \end{aligned} \quad (2.174)$$

The term  $D_H$  is called the Hubble volume. For the “all-sky” volume,  $\Theta^2 = 4\pi$ .

## 2.11 Probability of Line of Sight Intersection

For a non-evolving population of absorbers (constant proper density and constant cross-sectional area) that are simply carried along by cosmological expansion (i.e., the Hubble flow, see § 2.6), there are two effects governing the probability of line of sight intersection. The first arises because the proper distance between objects is increasing with decreasing redshift (by the factor  $D_c/(1+z)$ ). The second arises because the proper separation between objects increases as redshift decreases [by the factor  $D_T/(1+z) = D_A/(1+z)^2$ ]. Thus, the probability of intersection will decrease with decreasing redshift as absorbers flow radially and transversely away from one another.

In Fig. 2.14 a line of sight probe of the same region of space at two different arbitrary redshifts is shown. The co-moving distance interval is shown as the separation between the dashed lines at both epochs (recall that the co-moving distance is defined as the proper distance objects would have at  $z = 0$ ; it is a fixed quantity, see § 2.8.1). At lower redshift, the proper distance between objects is larger.

The incremental number of objects that will be intercepted over a radial proper distance element is

$$dN = \sigma n(z) dl_r = D_H n(z) \sigma \frac{dz}{(1+z)E(z)}, \quad (2.175)$$

where  $\sigma$  is the non-evolving cross sectional area,  $n(z)$  is the non-evolving proper number density, Eq. 2.95 has been employed to rewrite the radial proper distance element,  $dl_r$ , in terms of the redshift element,  $dz$ , and where  $E(z)$  is given by Eq. 2.80. The cross sectional area may also evolve with redshift (time), however, such evolution would not be causally connected to the relativistic dynamics governing the scale factor. From  $\rho_m(z) = \rho_m(1+z)^3$ , we have  $n(z) = n_0(1+z)^3$ , where  $n_0$  is the proper number density at the present time. Substituting into Eq. 2.175, gives the so-called

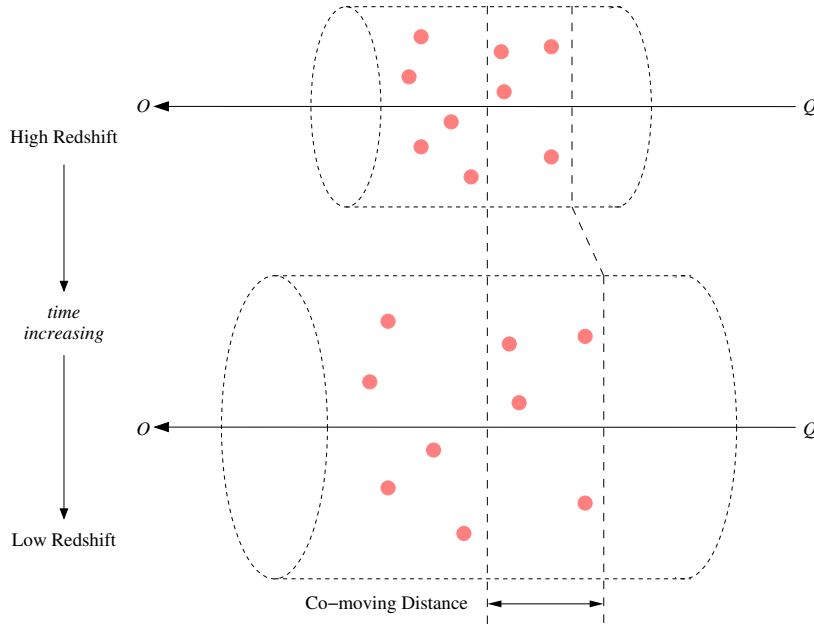


Figure 2.14: — An illustration of a pencil-beam survey through a representative cylinder of the universe populated by objects, such as absorbers. The upper panel represents earlier cosmic times at higher redshifts and the lower panel represents later cosmic times at lower redshifts. For illustration, the dashed vertical line on the left is the center of expansion. The distance between the two dashed lines gives the (unchanging) co-moving distance at each redshift. Note that the proper distance between objects has increased in both the line of sight and transverse directions.

redshift path density,

$$\frac{dN}{dz} = D_H n_0 \sigma \frac{(1+z)^2}{E(z)}. \quad (2.176)$$

The function of proportionality to  $dN/dz$  is the dimensionless probability of line of sight interception in a pencil beam survey, and is denoted,

$$\frac{dX}{dz} = \frac{(1+z)^2}{E(z)}, \quad (2.177)$$

This term is useful for characterizing cosmological evolution of the properties of objects detected in pencil-beam and quasar line-of-sight surveys; it describes the relationship between the combined increase of proper path length and proper projected absorber separation from the line of sight per

redshift element due to expansion. The term  $X$  is called the “absorption distance”. We then define the “absorption distance” as

$$X(z) = \int_0^z \frac{dX}{dz} dz. \quad (2.178)$$

A non-evolving population of absorbers with constant proper density and projected cross section will have a constant probability of being intersected by a line of sight probe as a function of  $X(z)$ , i.e.,  $dP/dX = (dP/dz)(dz/dX) = \text{constant}$ .

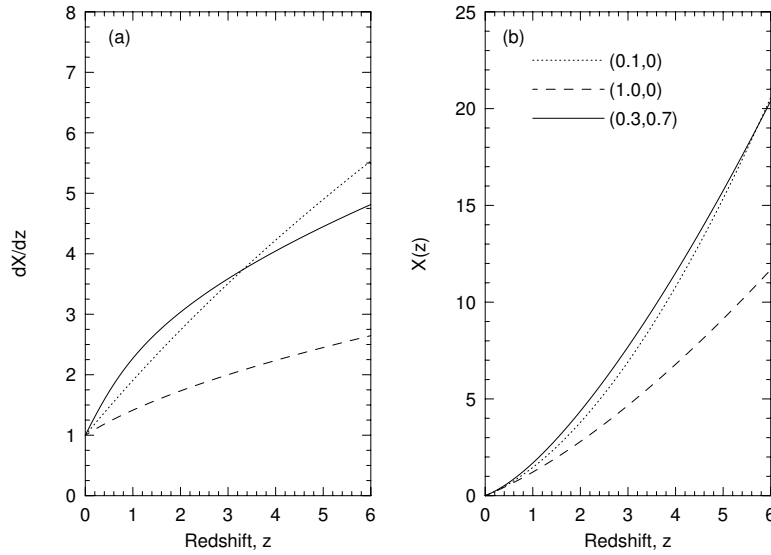


Figure 2.15: — (a) The dimensionless probability of line of sight intersection per redshift element as a function of redshift (Eq. 2.177). Three cosmologies are shown, denoted by  $(\Omega_m, \Omega_\Lambda)$ ; (i) the low-density (0.1,0), dotted; (ii) Einstein-de Sitter (1.0,0), dashed; and the concordance (0.3,0.7), solid. — (b) The absorption distance,  $X(z)$ , given by Eq. 2.178.

The dimensionless probability of line of sight intersection,  $dX/dz$ , and the absorption distance,  $X(z)$ , is shown in Figs. 2.15a and 2.15b, respectively, for the low-density, Einstein-de Sitter, and  $\Lambda$  Cosmologies. In a Friedmann cosmology ( $\Lambda = 0$ ), the expression for  $X(z)$  can be greatly simplified,

$$\frac{dX}{dz} = \frac{(1+z)}{\sqrt{1+2q_0z}}, \quad (2.179)$$



where  $E(z)$  is given by Eq. 2.83. Integrating gives

$$X(z) = \begin{cases} \frac{1}{2} [(1+z)^2 - 1] & q_0 = 0 \\ \frac{2}{3} [(1+z)^{3/2} - 1] & q_0 = 1/2 \end{cases} \quad (2.180)$$

If a population of objects has an evolving proper number density,  $n(z)$ , and evolving cross-sectional area,  $\sigma(z)$ , then the incremental number of absorbers intercepted along a line of sight over redshift element  $dz$  is,

$$\frac{dN}{dz} = D_H n(z) \sigma(z) \frac{dX}{dz} = D_H n(z) \sigma(z) \frac{(1+z)^2}{E(z)}, \quad (2.181)$$

Again, any such evolution would not be causally connected to the relativistic dynamics governing the scale factor; it would be evolution intrinsic to the objects. Writing this evolution as a function of redshift is only a means to parameterize any possible intrinsic evolution in terms of an observable.

Expressed in terms of the absorption distance,

$$\frac{dN}{dX} = \frac{dN}{dz} \frac{dz}{dX} = D_H n[X(z)] \sigma[X(z)], \quad (2.182)$$

which is a constant for non-evolving objects, i.e.,  $n(z)\sigma(z) = n_0\sigma_0$ . Thus, any evolution intrinsic to the objects, as probed via the product of the proper number density and the cross section, can be constrained directly from the measurement of the absorption distance path density,  $dN/dX$  (and therefore the measured  $dN/dz$ , the computation of which is provided in § 9).

## 2.12 Luminosities and Magnitudes

In this section, we introduce an additional cosmological distance, called the luminosity distance, and derive the redshift dependence of luminosity and surface brightness. We then review the Vega and AB photometric systems, and the  $K$ -correction, which accounts for the change in the rest-frame bandpass of an object as a function of redshift.

### 2.12.1 Luminosity Distance

When measuring the distance to an object based upon its observed flux, or when converting observed flux to luminosity, the distance applied in the conversion must account for the specific behavior of the inverse square law in the context of the relativistic dynamics of a curved expanding geometry.

This an operational definition, and the distance is called the luminosity distance,  $D_L$ .

Measured luminosity is energy delivered to the observer per unit time. Consider the bolometric luminosity,  $L$ , which is the emitted energy per unit time integrated over all wavelengths over all solid angle (having units  $\text{erg s}^{-1}$ ). Both energy and time are effected by the expansion, so that the observed luminosity is not equivalent to the emitted luminosity. If the energy of a photon at the redshifted emitter is  $E_e = hc/\lambda_e$ , then the energy of the photon received by an observer at  $z = 0$  is reduced such that

$$E_o(\lambda_o) = \frac{hc}{\lambda_o} = \frac{a(t_e)}{a_0} \frac{hc}{\lambda_e} = \frac{E_e(\lambda_e)}{1+z}. \quad (2.183)$$

In addition, the time interval between the arrival of photons at the observer is dilated relative to the time interval between the emission of the photons. From Eq. 2.108,

$$\Delta t_o = \frac{a_0}{a(t_e)} \Delta t_e = (1+z) \Delta t_e, \quad (2.184)$$

where  $\Delta t_o$  and  $\Delta t_e$  are the time intervals at the observer and emitter, respectively. This is equivalent to saying that the photon emission rate is higher at the source than the reception rate at the observer. Since the bolometric luminosity,  $L$ , is the integral over all wavelengths of the energy per unit time, we have

$$L(z) = \int \frac{E_o(\lambda)}{\Delta t_o} d\lambda = \frac{1}{(1+z)^2} \int \frac{E_e(\lambda)}{\Delta t_e} d\lambda = \frac{L}{(1+z)^2}, \quad (2.185)$$

where  $L(z)$  is the observed luminosity from an object at redshift  $z$ . The flux,  $F(z)$ , is the measured quantity after the luminosity from a source is spread over a sphere of co-moving area  $\mathcal{A} = 4\pi D_T^2$ , where  $D_T$  is the transverse co-moving distance given by Eqs. 2.124, 2.125 and 2.126 for  $\Omega_k = 0$ ,  $\Omega_k < 0$ , and  $\Omega_k > 0$ , respectively. Thus, the observed flux for an object at redshift  $z$  is

$$F(z) = \frac{L(z)}{4\pi D_T^2} = \frac{L}{4\pi D_T^2 (1+z)^2} = \frac{L}{4\pi D_L^2}, \quad (2.186)$$

which provides the definition of the luminosity distance

$$D_L = (1+z) D_T = (1+z)^2 D_A. \quad (2.187)$$

where  $D_A$  is the angular diameter distance given by Eq. 2.132.

The luminosity distance is shown in Fig. 2.16 for the low-density, Einstein-de Sitter, and  $\Lambda$  Cosmologies. The left axis gives the distance in Gigaparsecs for  $h = 0.7$ . The right axis gives the distance in units of the Hubble Distance, which is  $\sim 4.3$  Gpc for  $h = 0.70$ .

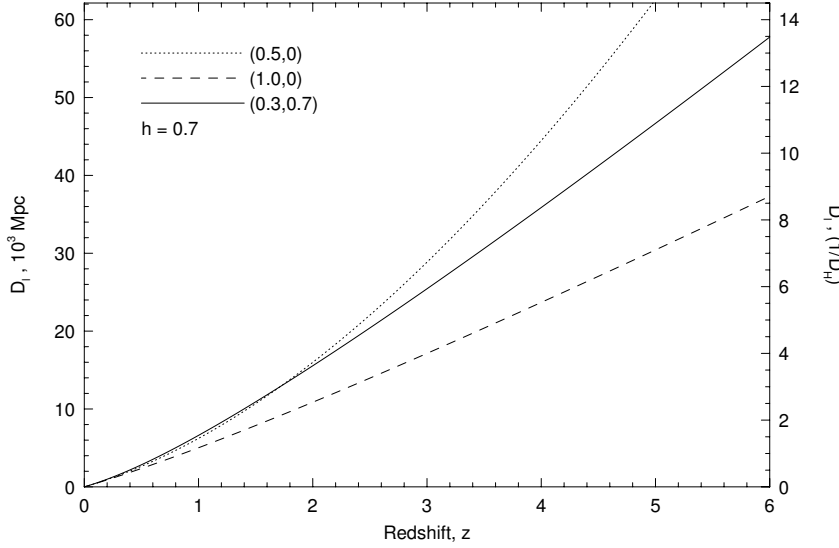


Figure 2.16: — The luminosity distance, given by Eq. 2.187. Three cosmologies are shown, denoted by  $(\Omega_m, \Omega_\Lambda)$ ; (i) the low-density (0.1,0), dotted; (ii) Einstein-de Sitter (1.0,0), dashed; and the  $\Lambda$  Cosmology (0.3,0.7), solid. The left hand scale provides the distance in Gigaparsecs for  $h = 0.7$ . The right hand scale provides the distance in units of  $D_H$ .

### 2.12.2 Surface Brightness

The intrinsic surface brightness of an extended object, such as a galaxy, is defined as its luminosity per unit area per  $4\pi$  steradians of solid angle,

$$\mu_0 = \frac{1}{4\pi} \frac{L}{d\mathcal{A}}, \quad (2.188)$$

as would be observed in the proximity of the object. The observed surface brightness of a high redshift extended object is defined as the collected energy per unit time per unit area of the collector (the telescope primary mirror). Thus, surface brightness is the observed flux,  $F(z)$ , per unit solid angle of the object,  $d\Omega$ , or

$$\mu(z) = \frac{F(z)}{d\Omega} = \frac{1}{d\Omega} \frac{L}{4\pi D_L^2}. \quad (2.189)$$

where Eq 2.186 has been substituted for  $F(z)$ . The proper area,  $d\mathcal{A}$ , on the object over a solid angle  $d\Omega$  is

$$d\mathcal{A} = d\Omega D_A^2, \quad (2.190)$$

where  $D_A$  is the angular diameter distance (Eq. 2.132). The expression for  $d\mathcal{A}$  follows from the same principle as the linear proper separations given by Eq. 2.133. Substituting for  $d\Omega$  in Eq. 2.189 yields

$$\mu(z) = \frac{D_A^2}{D_L^2} \left( \frac{1}{4\pi} \frac{L}{d\mathcal{A}} \right) = \frac{D_A^2}{D_L^2} \mu_0. \quad (2.191)$$

From Eq. 2.187,  $D_L/D_A = (1+z)^2$ , which yields

$$\mu(z) = \frac{\mu_0}{(1+z)^4}. \quad (2.192)$$

Note that the observed surface brightness is fully independent of the cosmological parameters; it depends only upon the evolution in the scale factor to the fourth power.

### 2.12.3 Magnitudes

In practice, bolometric fluxes are not the observed quantity, and one cannot compute the bolometric luminosity,  $L$ , of an object directly from Eq. 2.186. Normally, objects are measured using a filtered bandpass that is part of a photometric system comprising a suite of filtered bandpasses. These photometric systems are calibrated using the magnitude system. Magnitudes are unitless numbers on an inverted logarithmic scale that are based upon flux ratios. The zero points defined by the fluxes of standard objects must account for the filter bandpass response functions.

#### 2.12.3.1 Apparent Magnitude

The apparent magnitude,  $m$ , is defined as the ratio of the integrated flux of the object modulated by the filter response function to that of a standard source also modulated by the filter bandpass. For a non-cosmological object, the apparent magnitude in a bandpass  $y$  is defined as

$$m_y = -2.5 \log \left( \frac{\mathcal{F}_y}{\mathcal{F}_y^s} \right) \quad (2.193)$$

where the bandpass modulated flux of the observed object is

$$\mathcal{F}_y = \int_{\lambda_{y-}}^{\lambda_{y+}} R_y(\lambda) \lambda f_\lambda(\lambda) d\lambda \quad (2.194)$$

and the calibrated bandpass modulated flux of the standard source is

$$\mathcal{F}_y^s = \int_{\lambda_{y-}}^{\lambda_{y+}} R_y(\lambda) \lambda f_\lambda^s(\lambda) d\lambda \quad (2.195)$$

where  $f_\lambda$  and  $f_\lambda^s$  are the flux density of the object and the standard source, respectively, and where  $\lambda_{y-}$  and  $\lambda_{y+}$  are the lower and upper limits to the response function,  $R_y(\lambda)$ , of the bandpass  $y$  filter. The observed flux,  $F_\lambda$ , is related to the flux density  $f_\lambda(\lambda)$ , via

$$F(\lambda) = \lambda f_\lambda(\lambda), \quad (2.196)$$

where the units of  $F(\lambda)$  are  $\text{erg s}^{-1} \text{ cm}^{-2}$  and the units of  $f_\lambda(\lambda)$  are  $\text{erg s}^{-1} \text{ cm}^{-2} \text{ \AA}^{-1}$ . The response functions are the probability of transmission at each wavelength and obey

$$\int_{\lambda_{y-}}^{\lambda_{y+}} R_y(\lambda) d\lambda = 1. \quad (2.197)$$

Alternatively, the flux can also be written in terms of the frequency flux density  $\nu f_\nu(\nu)$ , where  $f_\nu(\nu)$  has units of  $\text{erg s}^{-1} \text{ cm}^{-2} \text{ Hz}^{-1}$ . Three useful relationships between  $f_\nu(\nu)$  and  $f_\lambda(\lambda)$ , where the first derives from flux conservation and the latter two follow from  $c = \nu\lambda$ , are

$$\begin{aligned} \nu f_\nu(\nu) &= \lambda f_\lambda(\lambda), \\ f_\lambda(\lambda) &= \frac{c}{\lambda^2} f_\nu(\nu), \\ \lambda f_\lambda(\lambda) d\lambda &= \frac{c}{\nu} f_\nu(\nu) d\nu, \end{aligned} \quad (2.198)$$

This latter relationship provides the substitution into Eqs. 2.194 and 2.195 if one prefers the frequency flux density integrated from  $\nu_- = c/\lambda_-$  to  $\nu_+ = c/\lambda_+$ .

### 2.12.3.2 Photometric Systems

There are two main photometric systems employed in the astronomical sciences, the Vega system and the AB system. There are a plethora of filter suites, including the Johnson-Cousins, Washington, Gunn, Sloan Digital Sky Survey, Hipparcos-Tycho, and *Hubble Space Telescope* WFPC2 sets. For a general review see Bessell (2005). For brevity, we employ the Johnson-Cousin *UBVRI* system for purposes of illustration.

The Vega system is calibrated using the flux density of the A0 V star Vega (or sometimes the mean of a sample of unreddened A0 V Pop I stars). The calibration flux density is the flux density that yields  $m_y = 0$  for all filter bandpasses (though it has been revised to  $m_y = 0.03$ ). Because A0 V stars do not have a flat flux density distribution, the calibration flux

density is different for each bandpass. For additional information see Bessell (1990). For information on the Sloan filter suite and calibration, see Smith et al. (2002).

For AB magnitudes, there is no physical standard source, but simply a definition of a hypothetical source with  $f_\nu = 3.63 \times 10^{-20} \text{ erg s}^{-1} \text{ cm}^{-2} \text{ Hz}^{-1}$  for all  $\nu$  (a flat frequency flux density distribution). This definition was chosen to give  $m_V(\text{AB}) = m_V$ , however the latest calibrations yield a difference of 0.044 magnitudes. This is not a flat flux density in wavelength,  $f_\lambda = 0.1092/\lambda^2 \text{ erg s}^{-1} \text{ cm}^{-2} \text{ \AA}^{-1}$  (where  $\lambda$  is substituted in units of angstroms). Because  $f_\nu$  is a constant, we have  $\mathcal{F}_y^s = f_\nu$  (Eq. 2.195), which yields

$$m_y(\text{AB}) = -2.5 \log \mathcal{F}_y - 48.60 \quad (2.199)$$

from the definition of apparent magnitude.

The standard Vega and AB flux density distributions,  $f_\lambda(\lambda)$ , are shown in Fig. 2.17. The Johnson–Cousins *UVBRI* bandpass response curves are superimposed (thick solid curves). Vega is shown as the thin solid curve (which exhibits absorption features), and the AB source is shown as the smooth dashed curve. Note that the curves are normalized (by definition for AB magnitudes) near the center of the response curve for the *V* filter. In fact, the AB system was defined such that the integral of  $R_V(\lambda)\lambda f_\lambda(\lambda)d\lambda$  is equivalent for Vega and the hypothetical AB source (however, refined measurements of Vega have slightly offset the two).

In Table 2.1, the central (effective) wavelength,  $\lambda_c$ , and the bandpass width,  $\Delta\lambda/\lambda_c$ , are listed for the Johnson–Cousins *UBVRI* filter suite. Also listed are the values of  $f_\nu(\nu_c)$  ( $\text{erg s}^{-1} \text{ cm}^{-2} \text{ Hz}^{-1}$ ) and  $f_\lambda(\lambda_c)$  ( $\text{erg s}^{-1} \text{ cm}^{-2} \text{ \AA}^{-1}$ ) defined at  $\lambda_c$  which yield  $m_y = 0$ . The values of the latter can be visually confirmed by inspection of Fig 2.17. The last column lists the magnitude difference between the Johnson–Cousins Vega system and the Johnson–Cousins AB system,  $m_y - m_y(\text{AB}) = \Delta m_y(\text{AB})$ , i.e., the quantity added to the Johnson magnitude in bandpass *y* to obtain the AB magnitude in that bandpass.

In imaging studies, one measures  $\mathcal{F}_y$  directly. In spectroscopic studies,  $\mathcal{F}_y$  must be computed using Eq. 2.194 from the measured flux density. In practice, imaging studies are more accurate because measuring the flux density spectroscopically is complicated by additional wavelength dependent transmission efficiencies (atmospheric, reddening, matching slit size to seeing, etc).

### 2.12.3.3 Absolute Magnitude and Luminosity

The absolute magnitude in bandpass *y*,  $M_y$ , is defined as the apparent magnitude that an observer would measure at a distance of 10 pc from

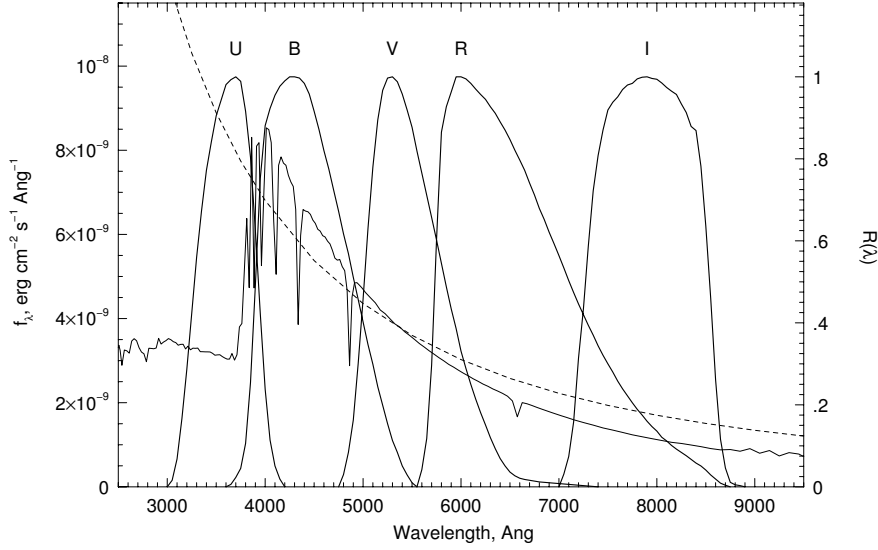


Figure 2.17: — The flux densities,  $f_\lambda$ , of Vega (thin solid curve) and the hypothetical AB source (dashed curve). Superimposed are the Johnson–Cousins *UBVRI* filter response curves normalized to unity at their peak transmissions. Note that integral to obtain  $\mathcal{F}^s$  for  $m_V$  is effectively equivalent to that for  $m_V(\text{AB})$ . The differences between the calibration magnitude of Vega and that of the AB magnitude are listed in Table 2.1.

the source. In a sense,  $M$  is a surrogate luminosity in that it normalizes observed flux to a standardized distance. To account for the finite bandpass, the luminosity density,  $L_\lambda$ , is employed,

$$L(\lambda) = \lambda L_\lambda(\lambda), \quad (2.200)$$

where  $L(\lambda)$  is in units  $\text{ergs s}^{-1}$ , and  $L_\lambda(\lambda)$  is in units  $\text{ergs s}^{-1} \text{\AA}^{-1}$ . The relationship between the flux density and the luminosity density is

$$f_\lambda(\lambda) = \frac{L_\lambda(\lambda)}{4\pi D^2}. \quad (2.201)$$

The conversion from  $L_\lambda(\lambda)$  to  $L_\nu(\nu)$  follows the relations for the flux density as given in Eq. 2.198.

In terms of luminosity, the apparent magnitude of a non-cosmological object in bandpass  $y$  can then also be written

$$m_y = -2.5 \log \left[ \int_{\lambda_{y-}}^{\lambda_{y+}} R_y(\lambda) \frac{\lambda L_\lambda(\lambda)}{4\pi D^2} d\lambda \right] + 2.5 \log F_y^s, \quad (2.202)$$

Table 2.1: Vega and AB Magnitude Data

Bandpass ( $y$ )	$\lambda_c$ [Å]	$\Delta\lambda/\lambda_c$	$f_\nu^s(\nu_c)$ [ $10^{-20}$ ]	$f_\lambda^s(\lambda_c)$ [ $10^{-9}$ ]	$\Delta m(\text{AB})$
U	3600	0.15	1.81	3.18	...
B	4400	0.22	4.26	6.60	-0.163
V	5500	0.16	3.64	3.61	-0.044
R	6400	0.23	3.08	2.26	+0.055
I	7900	0.19	2.55	1.23	+0.309

The absolute magnitude is obtained by setting  $D = 10$  pc,

$$M_y = -2.5 \log \left[ \int_{\lambda_{y-}}^{\lambda_{y+}} R_y(\lambda) \frac{\lambda L_\lambda(\lambda)}{4\pi(10\text{pc})^2} d\lambda \right] + 2.5 \log F_y^s, \quad (2.203)$$

The difference,  $m_y - M_y$ , is called the distance modulus

$$DM = 5 \log \left( \frac{D}{10 \text{ pc}} \right) = 5 \log D - 5, \quad (2.204)$$

where the distance to the object,  $D$ , is expressed in parsecs. Thus, if the apparent magnitude is measured in the rest frame of an object, the absolute magnitude can be computed from

$$M_y = m_y - DM, \quad (2.205)$$

If there is a measured characteristic absolute magnitude,  $M_y^*$ , for the bandpass, such as with galaxy luminosity functions, then the bandpass  $y$  absolute magnitude can be converted to the  $y$ -band luminosity using

$$M_y - M_y^* = -2.5 \log \left( \frac{L_y}{L_y^*} \right) \quad (2.206)$$

or more directly,

$$\frac{L_y}{L_y^*} = 10^{-0.4(M_y - M_y^*)} \quad (2.207)$$

Recent redshift surveys of galaxies (e.g., Faber et al., 2006) have reported that there is both redshift and bandpass (color) dependence on the values



of  $M^*$ . Thus, some care must be taken in obtaining luminosities for redshifted galaxies by invoking the correct characteristic absolute magnitude for the redshift and color of the galaxy. In terms of solar luminosity, the characteristic luminosity can be obtained from the sun's absolute magnitude for the bandpass  $y$ , i.e.,  $M_y^* - M_{\odot,y}$ .

#### 2.12.3.4 Luminosity and Fixed Bandpass

For cosmologically redshifted objects observed over a fixed filter bandpass, the observed wavelength or frequency interval defined by the bandpass will not span the same interval in the rest frame of the object. This follows directly from the relation  $\lambda_o/\lambda_e = a_0/a(t_e) = 1 + z$ , which shifts (and expands) the observed spectrum relative to the emitted spectrum.. Therefore, in the case of fixed bandpass observations, the bolometric luminosity (as discussed in § 2.12.1) does not apply.

Expressing the luminosity in terms of the luminosity density (Eq. 2.201), allows for conversions from the rest frame of the emitter to the observer frame for fixed bandpass at the observer. The observed flux,  $F(\lambda_o)$ , is

$$F(\lambda_o) = \lambda_o f_\lambda(\lambda_o) = \frac{\lambda_e L_\lambda(\lambda_e)}{4\pi D_L^2}, \quad (2.208)$$

where the luminosity distance, given by Eq. 2.187, is applied. Substituting  $\lambda_o = (1 + z)\lambda_e$  in the right hand side yields

$$f_\lambda(\lambda_o) = (1 + z) \frac{L_\lambda(\lambda_e)}{4\pi D_L^2}. \quad (2.209)$$

Similarly, from  $F(\nu_o) = \nu_o f_\nu(\nu_o)$ , and applying  $\nu_o = \nu_e/(1 + z)$ , we have

$$f_\nu(\nu_o) = \frac{1}{1 + z} \frac{L_\nu(\nu_e)}{4\pi D_L^2}. \quad (2.210)$$

(If you are wondering where the time dilation discussed in § 2.12.1 applies, recall that it is folded into the definition of the luminosity distance.)

Normally, the rest-frame luminosity density of an object is not known (though it can be computed from the observed flux density using Eqs. 2.209 and 2.210). Due to these shifts in bandpass from emitter frame to observer frame, one must apply a correction, called the  $K$  correction, to obtain the rest-frame apparent magnitude.

#### 2.12.4 The $K$ -Correction

Since the observed bandpass does not correspond to the bandpass in the rest frame for cosmologically redshifted objects, obtaining the absolute magnitude,  $M_y$  (Eq. 2.205) in a fixed bandpass is somewhat complicated. The

absolute magnitude requires the apparent magnitude measured in the object's rest frame,  $m_y$ . The “correction” term from the observed apparent magnitude to the rest-frame apparent magnitude is called the  $K$ -correction and it is defined through the relationship

$$M_y = m_y - DM = (m_y^z - K_y) - DM, \quad (2.211)$$

where  $m_y^z$  is the apparent magnitude of the redshifted object in the observer frame for bandpass  $y$ . Note that the distance modulus, DM, must be computed using the luminosity distance,  $DM = 5 \log D_L - 5$ .

There are two contributions to the  $K$  correction for an object at redshift  $z$ , both expressed as magnitudes. The first contribution arises from the fact that the observed, redshifted spectrum is stretched such that width of the bandpass in the rest-frame of the object is reduced by the factor  $1+z$ . This term is independent of the flux density distribution; even a flat distribution, i.e.,

$$f_\lambda(\lambda) = f_\lambda[\lambda/(1+z)], \quad (2.212)$$

where  $f_\lambda(\lambda)$  is the rest-frame flux density and  $f_\lambda[\lambda/(1+z)]$  is the observed flux density in the fixed bandpass  $y$ , would require a downward magnitude correction by the factor  $2.5 \log(1+z)$ . The second contribution is due to the band shifting and applies only when  $f_\lambda(\lambda) \neq f_\lambda[\lambda/(1+z)]$ . It accounts for the fact that the observed region of the redshifted spectrum in the fixed bandpass  $y$  is at shorter wavelengths in the rest frame of the object. This second correction is obtained by “redshifting” the rest-frame flux density into the observed bandpass and then computing the magnitude in the usual way.

In top panel of Fig 2.18, an example of a redshifted galaxy spectrum is shown for  $z = 0.6$  as observed through the Johnson–Cousins  $R$  bandpass. The rest-frame observation is shown in the lower panel of Fig 2.18. Note that the redshifted flux density distribution is observed in the object rest frame near 4000 Å. Also note that the fixed  $R$  bandpass covers a shorter wavelength range in the rest frame of the redshifted galaxy (as schematically shown in the lower panel with the dashed curve). From Eq. 2.193, the general expressions for the apparent magnitudes in bandpass  $y$  are

$$\begin{aligned} m_y &= -2.5 \log \left( \frac{\mathcal{F}_y}{\mathcal{F}_y^s} \right) \\ m_y^z &= -2.5 \log \left( \frac{\mathcal{F}_y^z}{\mathcal{F}_y^s} \right), \end{aligned} \quad (2.213)$$

where the calibrated bandpass modulated flux  $\mathcal{F}_y^s$  is given by Eq. 2.195, and  $\mathcal{F}_y^z$  is the observed bandpass modulated flux of the redshifted spectrum.

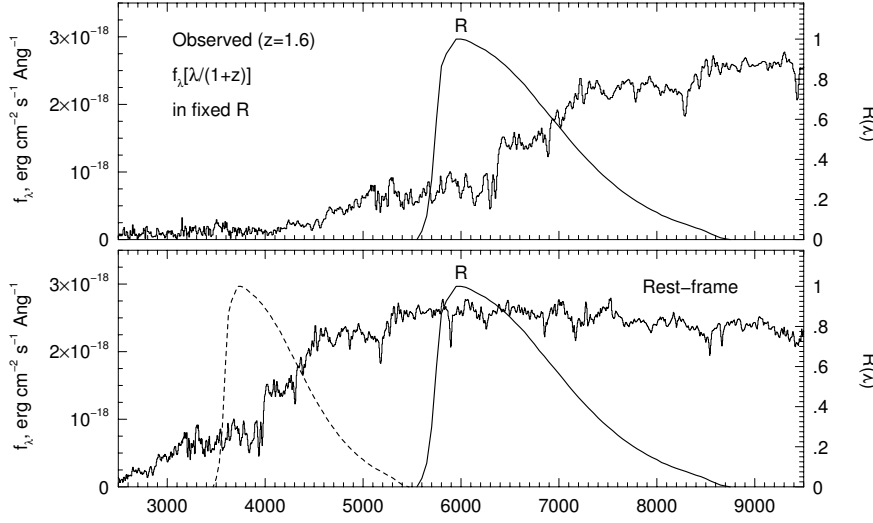


Figure 2.18: — (upper) The observed spectrum of a target galaxy in the Johnson–Cousins  $R$  filter, which is superimposed. The spectrum is observed to have redshift  $z = 0.6$  so that the observed flux density for fixed bandpass is  $f_\lambda[\lambda/(1+z)]$  in the rest frame of the galaxy. In the  $R$  bandpass, note that the  $z = 0.6$  object is being observed in its rest frame near  $4000 \text{ \AA}$ . — (lower) The same spectrum as observed in the rest frame with the  $R$  filter superimposed (solid curve). The dashed curve schematically shows the window of the  $R$  band in the rest frame of the redshifted galaxy in the upper panel. Note that the bandpass width is reduced by the factor  $1+z$ , so that the observed magnitude,  $m_R^z$ , will be too large by the factor of  $2.5 \log(1+z)$ .

The integrals for  $\mathcal{F}_y$  and  $\mathcal{F}_y^z$  are explicitly written

$$\begin{aligned} \mathcal{F}_y &= \int_{\lambda_{y-}}^{\lambda_{y+}} R_y(\lambda) \lambda f_\lambda(\lambda) d\lambda \\ \mathcal{F}_y^z &= \int_{\lambda_{y-}}^{\lambda_{y+}} R_y(\lambda) \lambda f_\lambda[\lambda/(1+z)] d\lambda, \end{aligned} \tag{2.214}$$

where  $f_\lambda(\lambda)$  is the flux density in the rest frame of the object. The rest-frame magnitude,  $m_y$ , is computed from the integral as illustrated in the lower panel of Fig 2.18 using the rest-frame flux density,  $f_\lambda(\lambda)$ , spanning the fixed bandpass. The observed magnitude,  $m_y^z$ , is obtained from the integral as illustrated in the upper panel of Fig 2.18 using the flux density shifted into the fixed bandpass,  $f_\lambda[\lambda/(1+z)]$ . From Eq. 2.211, the  $K$

correction is

$$K_y = 2.5 \log(1 + z) + (m_y^z - m_y), \quad (2.215)$$

where the bandpass correction term  $2.5 \log(1 + z)$  has been hand inserted. Substituting Eq 2.213 for the definitions of  $m_y^z$  and  $m_y$ , yields

$$K_y = 2.5 \log(1 + z) + 2.5 \log \left( \frac{\mathcal{F}_y}{\mathcal{F}_y^z} \right). \quad (2.216)$$

$K_y$  and  $m_y^z$  are applied to Eq. 2.211 to obtain the absolute magnitude,  $M_y$ , in the  $y$  bandpass (being sure to use the luminosity distance,  $D_L$ , to obtain the distance modulus,  $DM$ ). Note that the calibration terms,  $\mathcal{F}_y^s$ , have canceled in Eq. 2.216.

It has been implied throughout that the rest-frame flux density distribution is well known in order to compute the  $K$  correction. This is not normally the case. Magnitudes are usually measured directly using aperture photometry from imaging data, and not using the formalism described here for photometric spectroscopic data. Thus, for the computation of the  $K$  correction, the  $f_\lambda$  distribution must be estimated based upon additional information about the object (if any exists). Measuring the magnitudes in multiple bands can provide colors, i.e.,  $m_x - m_y$ , that can then be compared to a library of standard  $f_\lambda$  distributions in order to make a judicious estimate. A second piece of helpful information would be the object morphology in the case of galaxies, though this is a much less robust indicator.

#### 2.12.4.1 Transferring Passbands

Often one measures an object in bandpass  $y$ , but desired to measure the absolute magnitude in rest frame of bandpass  $x$ ,

$$M_x = m_x - DM = (m_y^z - K_{xy}) - DM, \quad (2.217)$$

where  $m_x$  is the rest-frame apparent magnitude in bandpass  $x$ ,  $m_y^z$  is the observed apparent magnitude in bandpass  $y$ , and  $K_{xy}$  is the  $K$  correction to convert from  $m_y^z$  to  $m_x$ .

A judicious choice of filter can result in a small  $K$  correction. If the observed bandpass  $y$  is chosen such that its central wavelength and bandwidth is similar to that of bandpass  $x$  in the rest frame of the object, then the  $K$ -correction can be significantly minimized. However, there is still an additional correction required to transfer the zero point of bandpass  $y$  to that of bandpass  $x$ . This correction factor is called the color term.

Consider a  $z = 0.6$  galaxy observed in the Johnson-Cousins  $R$  bandpass for which the desired quantity is the absolute magnitude in the  $B$  bandpass,  $M_B$  (in this example  $x = B$  and  $y = R$ ). In the upper-left panel

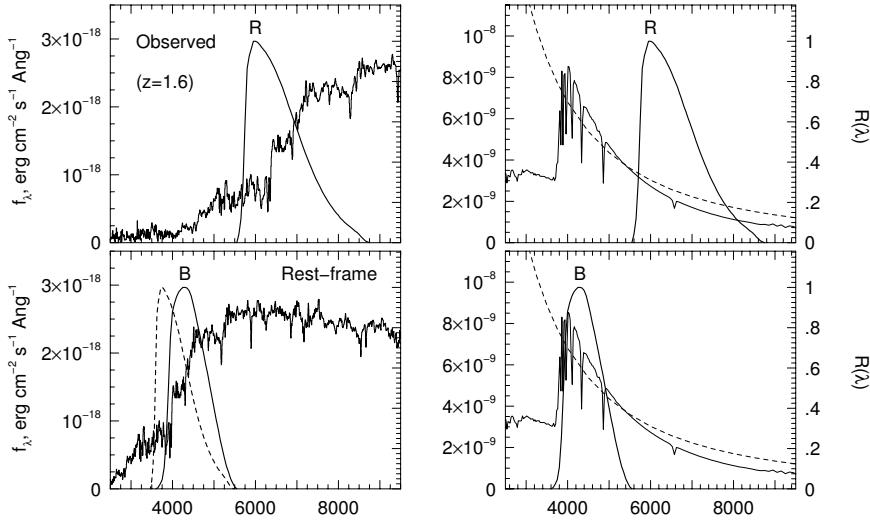


Figure 2.19: — An example object that is observed in the Johnson-Cousins  $R$  filter, but for which the absolute magnitude is desired in the Johnson-Cousins  $B$  filter, i.e.,  $M_B$ . — (upper left) The observed spectrum of a  $z = 0.6$  target galaxy in the Johnson-Cousins  $R$  filter, which is superimposed. — (lower left) The same spectrum as if it were observed in the rest frame in the Johnson-Cousins  $B$  filter, which is superimposed as the solid curve. The overlap of the  $B$  filter is somewhat similar to that of the  $R$  filter in the rest frame of the galaxy, as shown schematically with the dashed curve. — (right panels) The calibration sources, Vega (thin solid curve) and the hypothetical AB (dashed curve) with the  $R$  and  $B$  filters superimposed. These provide the so-called color term for the transfer from the  $R$  band zero point to the  $B$  band zero point.

of Fig 2.19, an example of a redshifted galaxy spectrum is shown for at  $z = 0.6$  as observed through the Johnson-Cousins  $R$  bandpass. The rest-frame observation in the  $B$  bandpass is shown in the lower-left panel of Fig 2.19. The  $B$  filter response is superimposed as the solid curve. Also shown schematically, is the  $R$  filter response as observed in the rest frame of the galaxy (dashed curve). In this example, the  $K_{xy}$  correction is the transfer from the observed  $R$  band magnitude of the redshifted galaxy to the  $B$  band in the rest frame of the galaxy. This transfer must account for the different zero points in the  $R$  and  $B$  bandpasses, as illustrated in the right-hand panels of Fig 2.19.

From Eq. 2.193, the general expressions for the rest-frame apparent magnitude in bandpass  $x$  and the observed apparent magnitude in bandpass

$y$  are

$$\begin{aligned} m_x &= -2.5 \log \left( \frac{\mathcal{F}_x}{\mathcal{F}_x^s} \right) \\ m_y^z &= -2.5 \log \left( \frac{\mathcal{F}_y^z}{\mathcal{F}_y^s} \right), \end{aligned} \quad (2.218)$$

where the terms have the usual meanings. The integrals for  $\mathcal{F}_x$  and  $\mathcal{F}_y^z$  are explicitly written

$$\begin{aligned} \mathcal{F}_x &= \int_{\lambda_{x-}}^{\lambda_{x+}} R_x(\lambda) \lambda f_\lambda(\lambda) d\lambda \\ \mathcal{F}_x^s &= \int_{\lambda_{x-}}^{\lambda_{x+}} R_x(\lambda) \lambda f_\lambda^s(\lambda) d\lambda \end{aligned} \quad (2.219)$$

and for the calibration terms  $\mathcal{F}_x^s$  and  $\mathcal{F}_y^s$  are written

$$\begin{aligned} \mathcal{F}_y^z &= \int_{\lambda_{y-}}^{\lambda_{y+}} R_y(\lambda) \lambda f_\lambda[\lambda/(1+z)] d\lambda \\ \mathcal{F}_y^s &= \int_{\lambda_{y-}}^{\lambda_{y+}} R_y(\lambda) \lambda f_\lambda^s(\lambda) d\lambda, \end{aligned} \quad (2.220)$$

where  $f_\lambda(\lambda)$  is the flux density in the rest frame of the object.

From Eq. 2.211, the  $K$  correction is  $K_{xy} = 2.5 \log(1+z) + (m_y^z - m_x)$ , which yields

$$K_{xy} = 2.5 \log(1+z) + 2.5 \log \left( \frac{\mathcal{F}_x}{\mathcal{F}_y^z} \right) + 2.5 \log \left( \frac{\mathcal{F}_y^s}{\mathcal{F}_x^s} \right) \quad (2.221)$$

which is applied in Eq. 2.217 to obtain  $M_x$ . Note the right-most term (the calibration terms do not cancel out), which is called the color term.

## References

- Bessell, M. S. 1990, “UBVRI Passbands” *PASP*, 102, 1181
- Bessell, M. S. 2005, “Standard Photometric Systems” *ARA&A*, 43, 293
- Burles, S., Nollett, K. M., & Turner, M. S. 2001, “Big Bang Nucleosynthesis Predictions for Precision Cosmology,” *ApJL*, 552, L1

- Carlberg, R. G., Yee, H. K. C., & Ellingson, E. 1997, "The Average Mass and Light Profiles of Galaxy Clusters," *ApJ*, 478, 462
- Carroll, S. M. Press, W. M., & Turner, E. L. 1992, "The Cosmological Constant," *ARA&A*, 30, 499
- Davis, T. M., & Lineweaver, C. H. 2004, "Expanding Confusion: Common Misconceptions of Cosmological Horizons and the Superluminal Expansion of the Universe," *Publications of the Astronomical Society of Australia*, 21, 97
- Faber, S. M., Willmer, C. N. A., Wolf, C., et al. 2006, "Galaxy Luminosity Functions to  $z \sim 1$ : DEEP2 vs. COMBO-17 and Implications for Red Galaxy Formation," *ApJ*, (astro-ph/050641)
- Halverson, N. W., et al. 2002, "Degree Angular Scale Interferometer First Results: A Measurement of the Cosmic Microwave Background Angular Power Spectrum," *ApJ*, 568, 38
- Hanany, S., et al. 2000, "MAXIMA-1: A Measurement of the Cosmic Microwave Background Anisotropy on Angular Scales of  $10'$ – $5^\circ$ ," *ApJL*, 545, L5
- Harrison, E. 1993, "The Redshift–Distance and Velocity–Distance Law," *ApJ*, 403, 28
- Hogg, D. 1999, "Distance Measures in Cosmology" (astro-ph/9905116).
- Netterfield, C. B., et al. 2002, "A Measurement by BOOMERANG of Multiple Peaks in the Angular Power Spectrum of the Cosmic Microwave Background," *ApJ* 571, 604
- Oke, J. B., & Gunn, J. E. 1983, "Secondary Standard Stars for Absolute Spectrophotometry," *ApJ*, 266, 713
- Peebles, J. 1996, "Principles of Physical Cosmology," (Princeton University Press : Princeton)
- Percival, W. J., et al. 2002, "Parameter Constraints for Flat Cosmologies from Cosmic Microwave Background and 2dFGRS Power Spectra," *MNRAS*, 337, 1068
- Perlmutter, S., et al. 1999, "Measurements of Omega and Lambda from 42 High-Redshift Supernovae," *ApJ*, 517, 565

- Schmidt, B. P., et al. 1998, “The High-Z Supernova Search: Measuring Cosmic Deceleration and Global Curvature of the Universe Using Type Ia Supernovae,” *ApJ*, 507, 46
- Smith, J. A., et al. 2002, “The u’g’r’i’z’ Standard-Star System,” *AJ*, 123, 2121
- Smette, A., Surdej, J., Shaver, P. A., Foltz, C. B., Chaffee, F. H., Weymann, R. J., Williams, R. E., & Magain, P. 1992, “A Spectroscopic Study of UM 673 A and B - On the Size of Lyman-alpha Clouds,” *ApJ*, 389, 39
- Sievers, J. L., et al. 2003, “Cosmological Parameters from Cosmic Background Imager Observations and Comparisons with BOOMERANG, DASI, and MAXIMA,” *ApJ*, 591, 599
- Spergel, D. N., et al. 2003, “First-Year Wilkinson Microwave Anisotropy Probe (WMAP) Observations: Determination of Cosmological Parameters,” *ApJS*, 148, 175
- Dodelson, S., et al. 2002, “The Three-Dimensional Power Spectrum from Angular Clustering of Galaxies in Early Sloan Digital Sky Survey Data,” *ApJ*, 572, 140
- Turner, M. S. 2002a, “The New Cosmology,” *International Journal of Modern Physics A*, 17, 3446
- Turner, M. S. 2002b, “Making Sense Of The New Cosmology,” (astro-ph/0202008 )
- Turner, M. S. 2002c, “The New Cosmology: Mid-term Report Card for Inflation,” (astro-ph/0212281)
- Turner, M. S. 2002, “The Case for  $\Omega_m = 0.33 \pm 0.035$ ,” *ApJL*, 576, L101
- Turner, M. S. 2001a, “A Sober Assessment of Cosmology at the New Millennium,” *PASP*, 113, 653
- Turner, M. S. 2001b, “Dark Energy and the New Cosmology,” (astro-ph/0108103)